Extended Lobes in AGN and Ultrarelativistic Particles

Lukasz Stawarz

KIPAC/SLAC, Stanford University

Radio Lobes in AGN

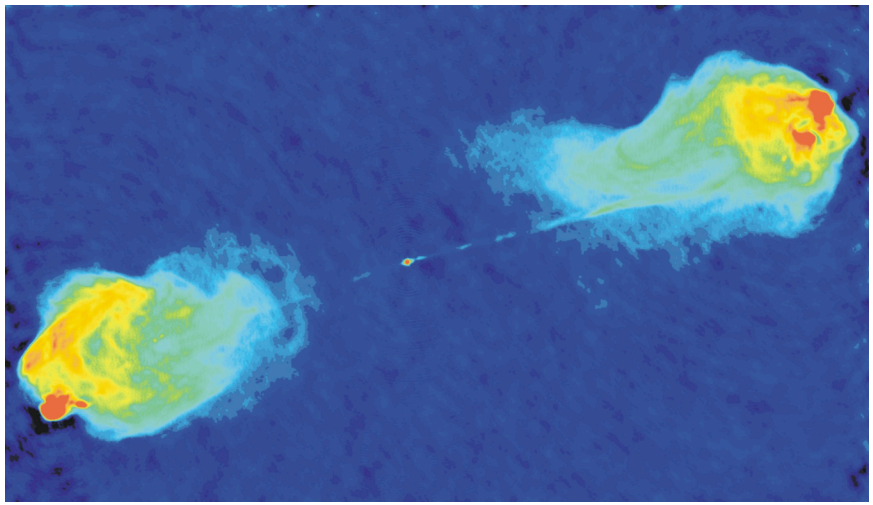

Carilli & Barthel 96: 5 GHz image of Cygnus A with 0.4" resolution made with the VLA (courtesy R. Perley).

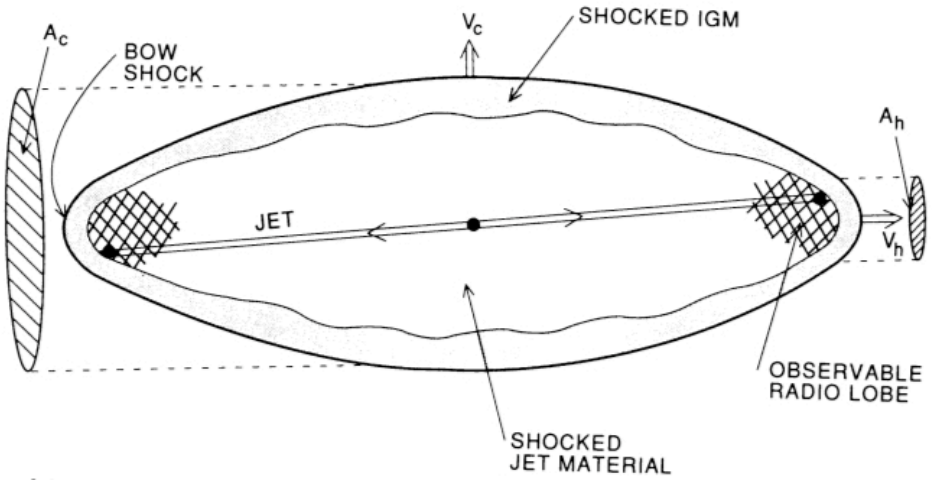

Begelman & Cioffi 89: model for classical doubles.

Cygnus A was the first object recognized as a double radio source (Jennison & Das Gupta 53), and identified with the first ultra-luminous active galaxy (Baade & Minkowski 54). The enormous energy involved was initially explained within a colliding galaxy scenario (Baade & Minkowski 54, Minkowski & Greenstein 1954), but the double nature of the radio source, stretching outside the optical object, was puzzling.

Since its discovery, Cygnus A has played a fundamental role in the development of jet theory for powering the double structures in powerful radio galaxies (the `beam' or `jet' model for powering double radio sources by Blandford & Rees 74 and Scheuer 74). The Cygnus A jet itself was suggested in early VLBI observations of the nucleus (Kellermann et al. 75, 81), and finally revealed in detail by the first high dynamic range images of the source with the VLA (Perley et al. 84).

Extended, Diverse

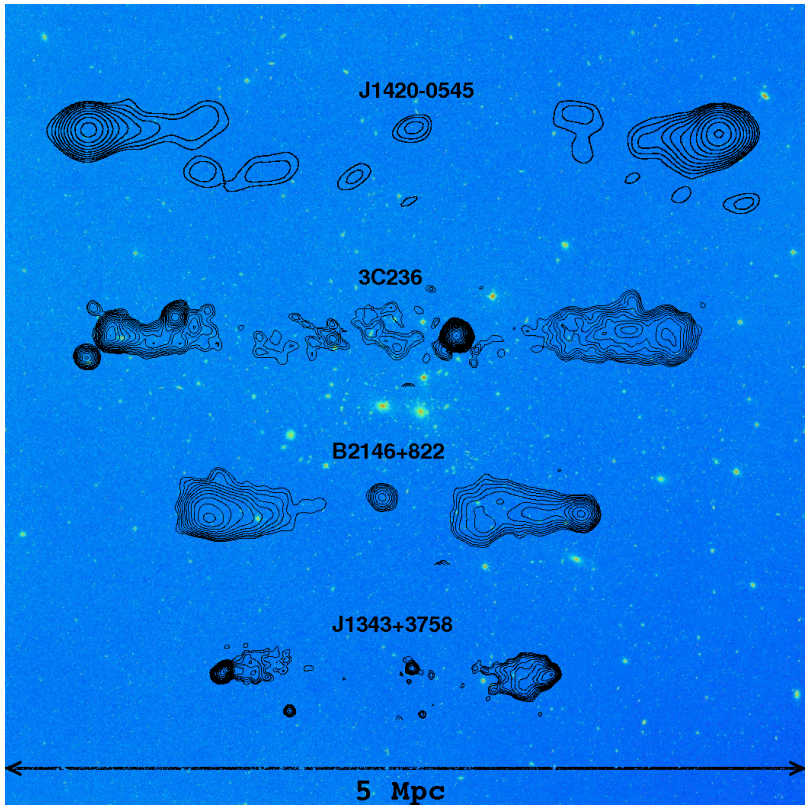

Machalski et al. 08: J1420-0545 radio source with an angular size of 17.4', identified with an optical galaxy at z = 0.3067. Thus, the projected linear size of the radio structure is 4.69 Mpc (for the assumed cosmology H_0 = 71 km s^{-1} Mpc^{-1}, Ω_m = 0.27, and Ω_Λ = 0.73).

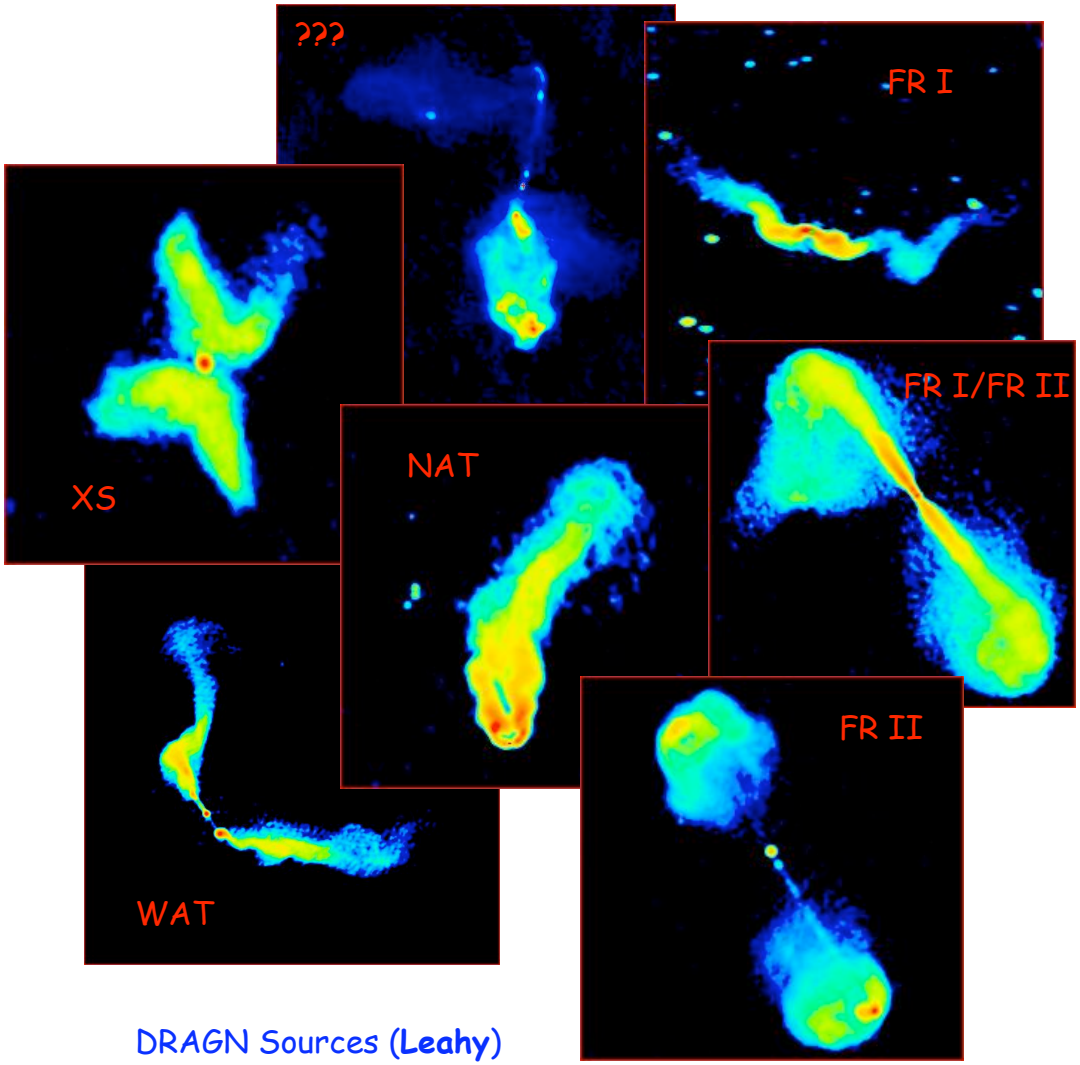

DRAGN Sources (**Leahy**)

The most compact lobes: LS ~ 0.1-1 kpc (GPS/CSO objects)

Complex Radio Morphologies

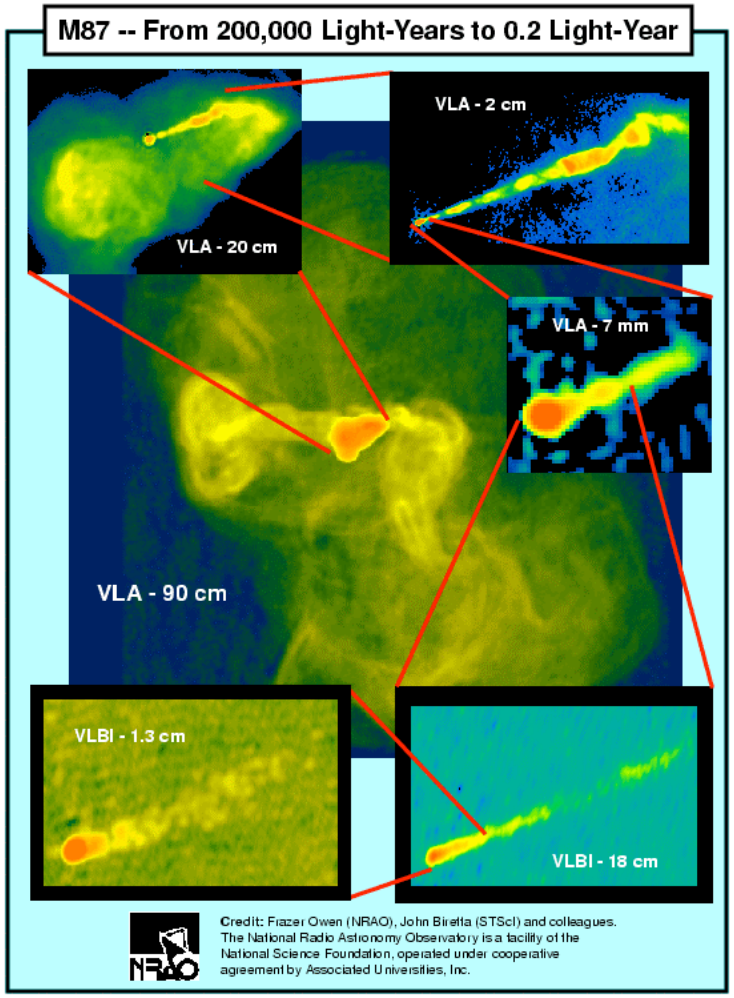

Complex large-scale (tens of kpc) structure of M87 radio galaxy (**Owen et al. 89**)

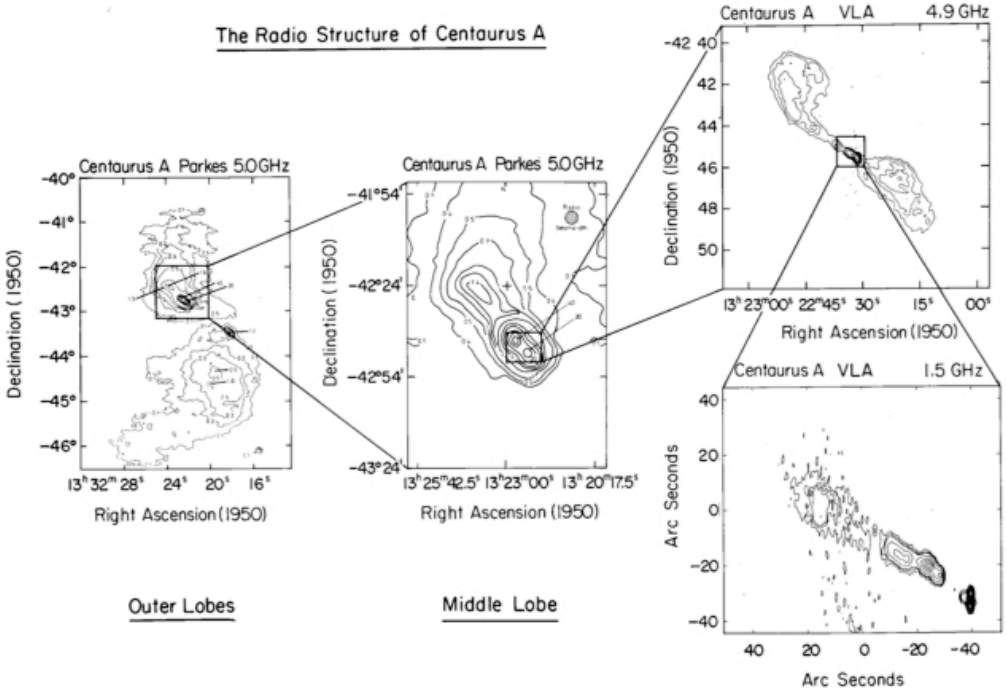

Complex large-scale (hundreds of kpc) structure of Centaurus A radio galaxy (**Morganti et al. 99**)

Complex Magnetic Topology

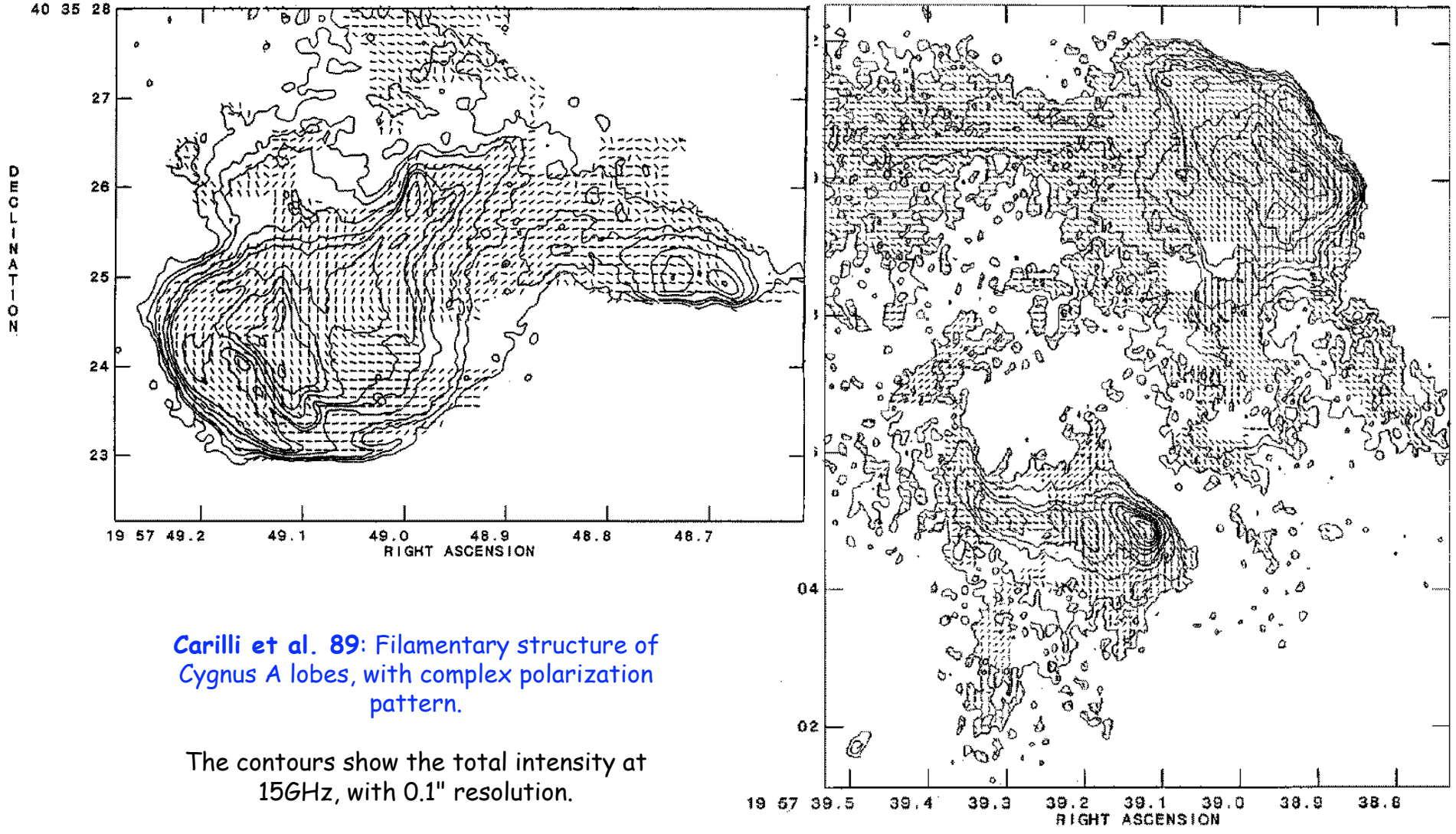

Carilli et al. 89: Filamentary structure of Cygnus A lobes, with complex polarization pattern.

The contours show the total intensity at 15GHz, with 0.1" resolution.

Radio Lobes in X-rays

IC/CMB emission of the extended lobes in radio galaxies was expected to be detected in X-rays (Harris & Grindlay 79). Indeed, ASCA and ROSAT resolved and detected the extended lobes of Fornax A (Kaneda et al. 95, Feigelson et al. 95).

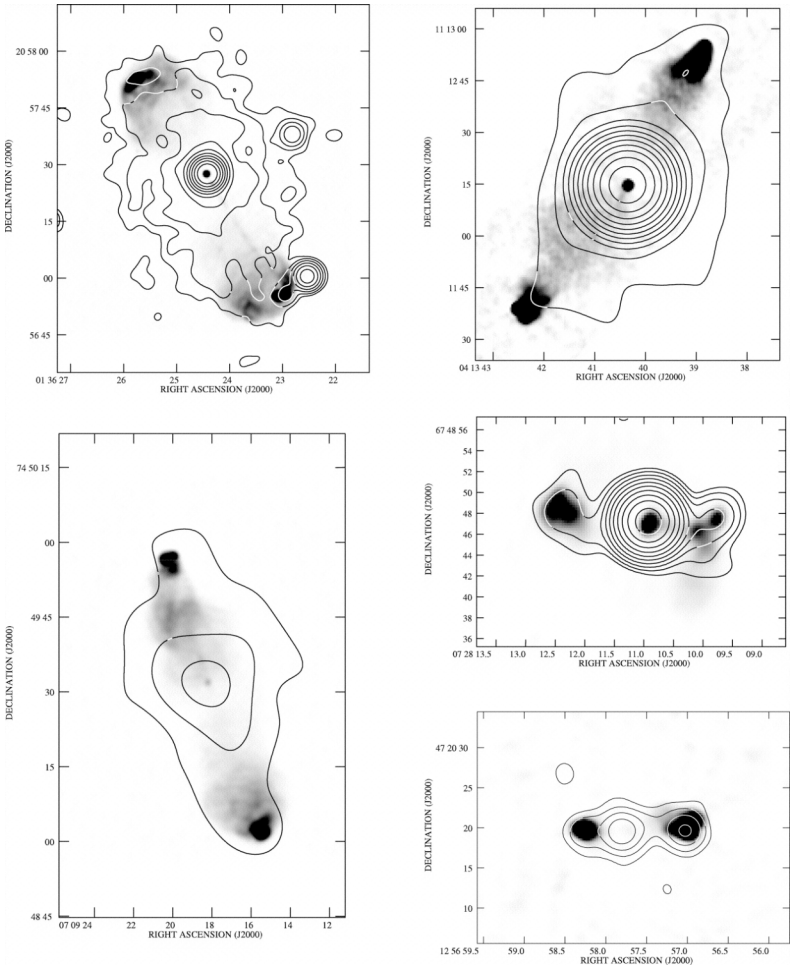

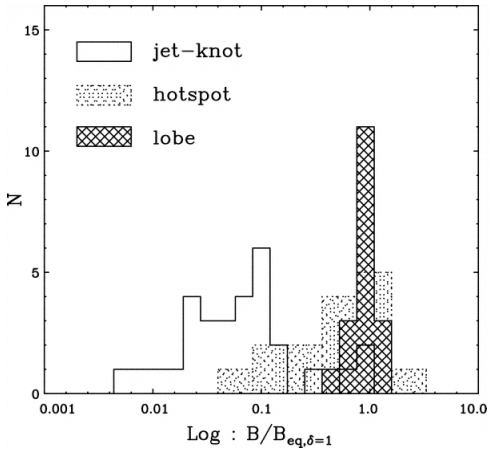

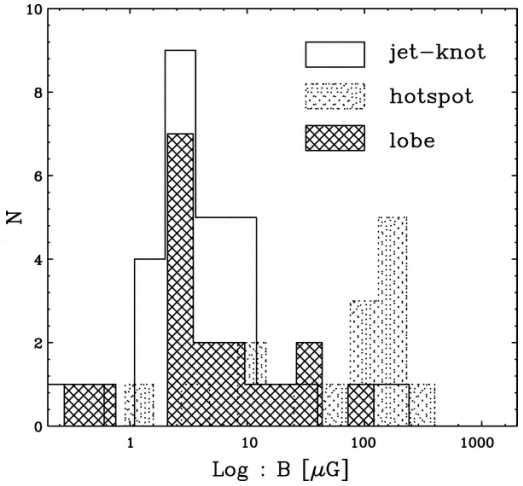

Kataoka & Stawarz 05, Croston et al. 05 and ref. therein: Chandra and XMM Newton enabled a systematic investigation of the IC/CMB emission of the extended lobes in X-rays. Such studies revealed that the radio lobes are close to the minimum energy condition (regarding strictly radiating ultrarelativistic electrons and magnetic field with the intensity B ~ 1-100 μG).

No thermal emission due to hot diffuse gas has been detected in X-rays. The resulting upper limits for the gas number density within the lobes are in agreement with the constraints obtained from the depolarization studies ($n_g < 10^{-4}$ cm^{-3}).

Radio Lobes in Gamma-rays?

Cheung 07: IC/CMB emission from the extended lobes of Cen A (and other radio galaxies) should be detected by GLAST/LAT at GeV photon energies, depending on the maximum energies of lobes' electrons. In addition, lobes of Cen A may be even resolved by GLAST/LAT.

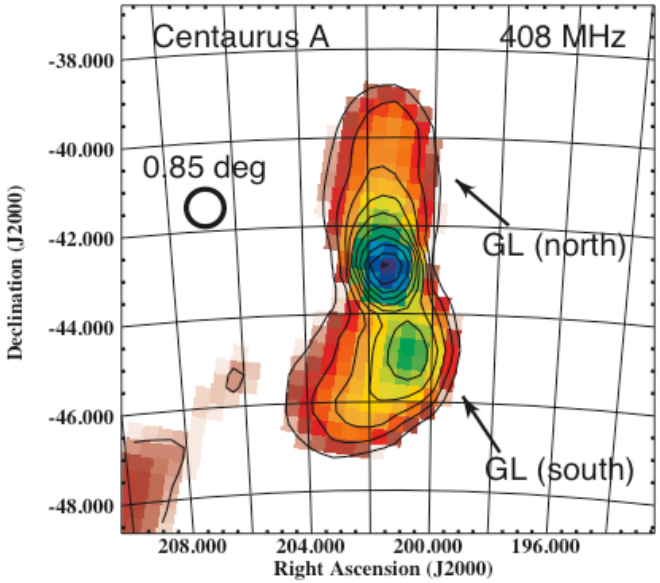

Radio image of Cen A at 0.85deg resolution (comparable to the expected GLAST/LAT angular resolution).

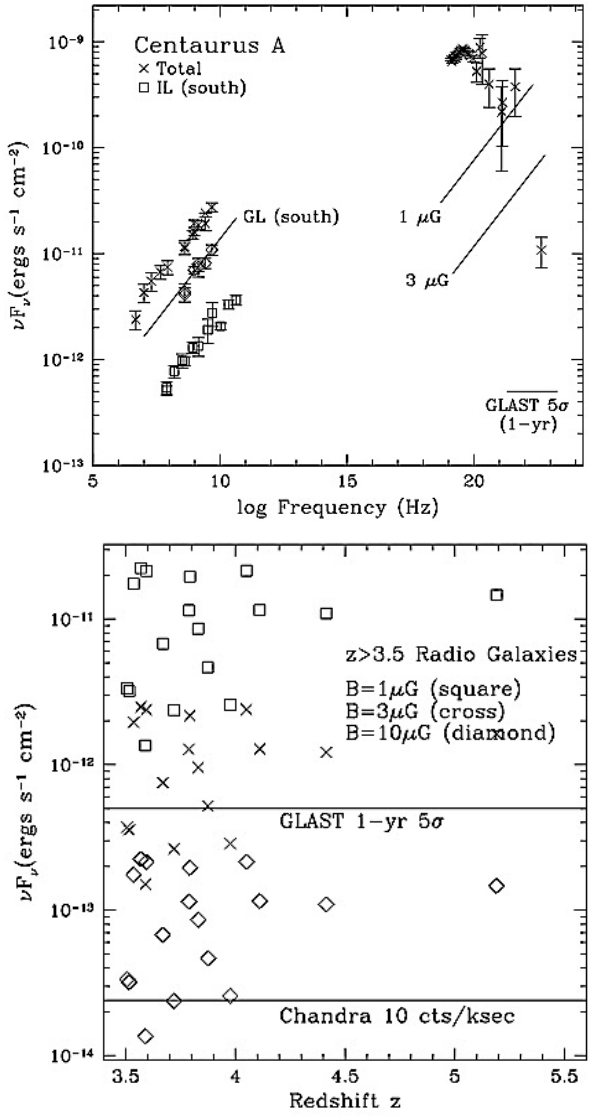

[Right, Upper] SEDs of the multiple components of the Cen A radio source. The data points at $>10^{18}$ Hz are the integrated detections with CGRO with lines indicating the expected IC/CMB spectra of the southern giant lobe for different average magnetic fields. **[Right, Lower]** X-ray and gamma-ray flux predictions for 17 of the highest redshift radio galaxies.

Probing EBL?

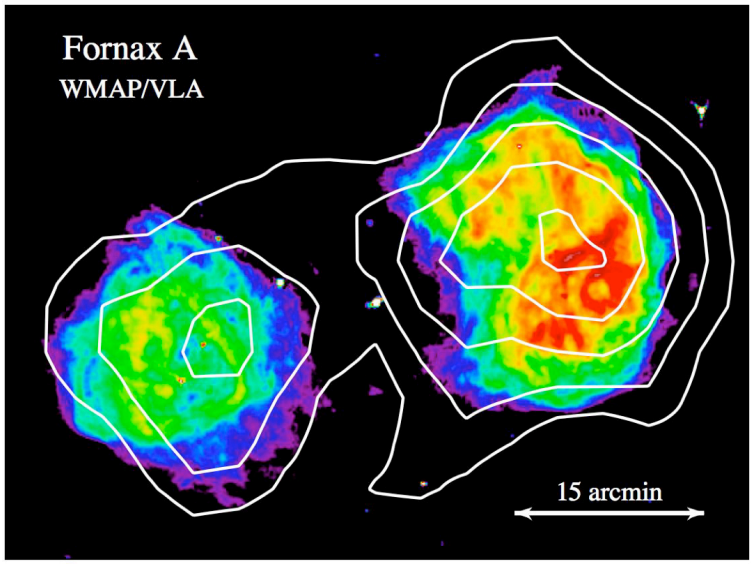

The 1.5 GHz VLA (color; Fomalont et al. 89) and 61 GHz WMAP (contours; Hinshaw et al. 07) images of Fornax A radio galaxy.

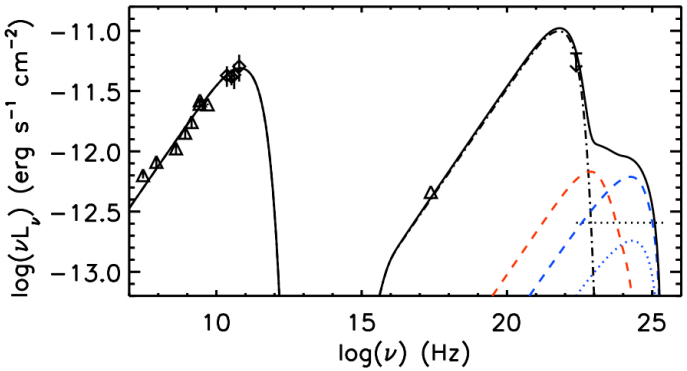

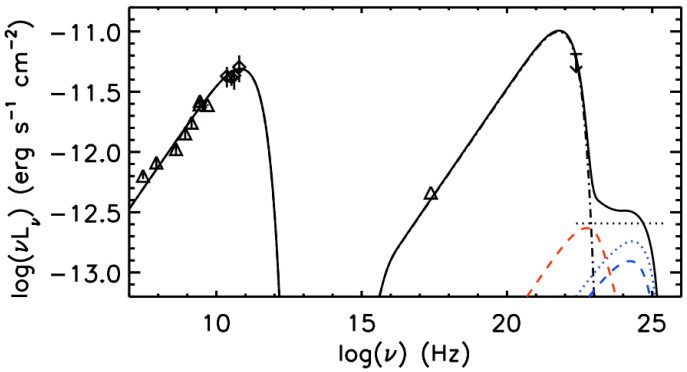

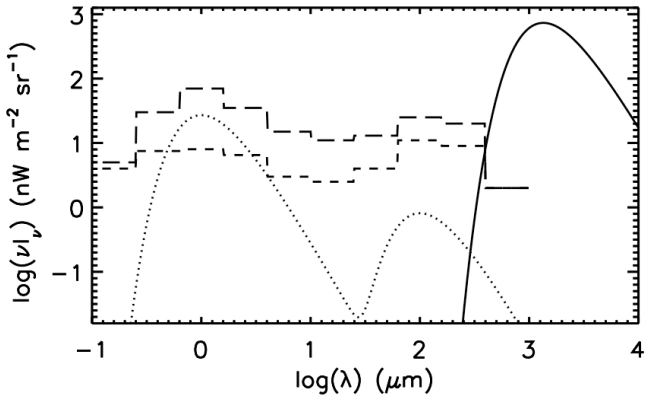

Georganopoulos et al. 08: The radio, WMAP, and X-ray flux from both radio lobes of Fornax A, as well as the EGRET upper limit. The solid line is the model SED, resulting from a magnetic field of $B \sim 2\ \mu G$, and a power law EED with slope $p = 2.3$ and maximum Lorentz factor $\gamma_{max} \sim 10^5$. We also plot the IC due to the CMB (dot-dash line), the CIB and COB (red and blue broken line), as well as the maximum expected level of the IC emission due to the optical photons of the host galaxy (dotted blue line). The black dotted line marks the 2 year, 5 σ Fermi/LAT sensitivity limit. The lower (upper) panel corresponds to the low (high) level EBL.

Giant Lobes of Cen A

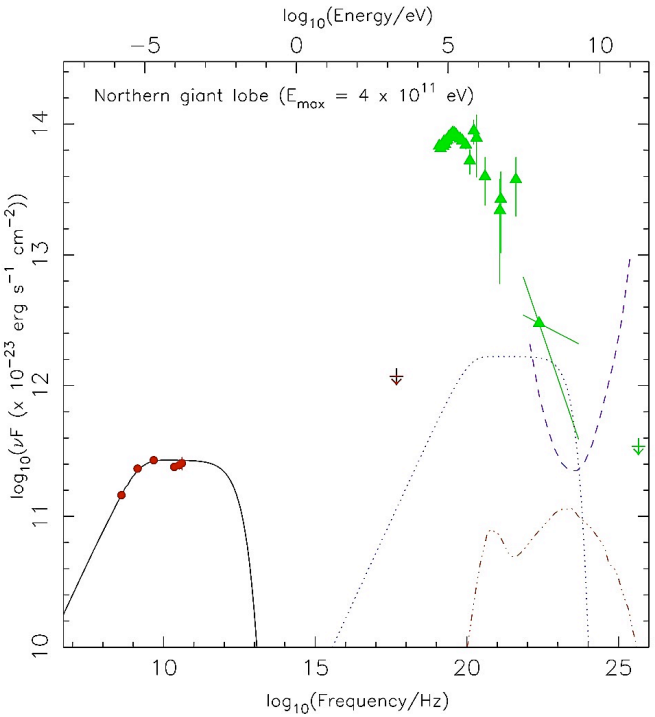

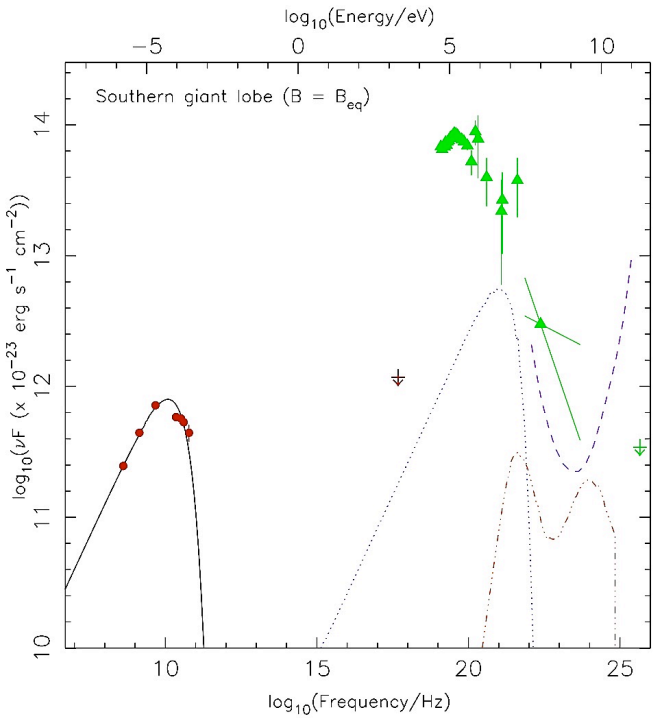

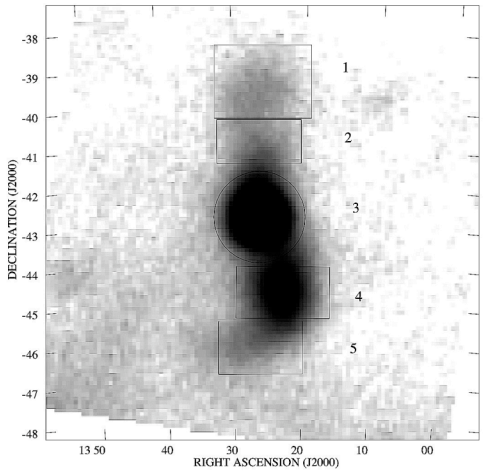

Hardcastle et al. 09: WMAP maps of giant lobes in Centaurus A radio galaxy indicate presence of (at least) 0.1 TeV energy electrons. These electrons should inverse-Compton upscatter background photons (CMB and EBL) to the observed GeV energies. The implied lobes' lifetime is ~ 30 Myr.

Middle Lobe of Cen A

Kraft et al. 09

Northern Middle Lobe of Cen A:
t_{life} ~100 Myrs

Thermal X-ray knots (most likely shock heated by the jet):
$n_g \sim 0.01$ cm^{-3}
$p_{th} \sim 2 \times 10^{-11}$ cgs >> p_{NML}
$M_g \sim 10^6$ M_{sol} each,
$E \sim (3 - 10) \times 10^{54}$ ergs each,
$t_{life} \sim 3$ Myr

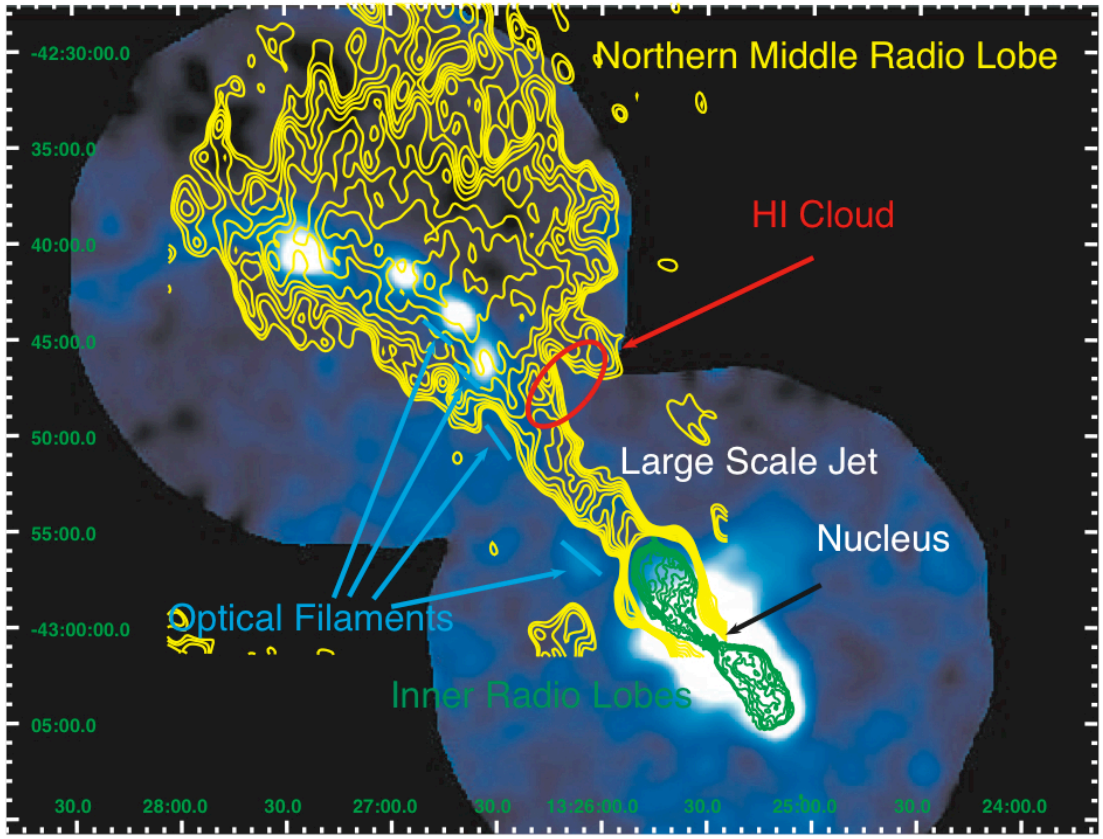

Exposure corrected, Gaussian smoothed XMM-Newton image of the inner jet/lobe and NML regions of Cen A. The inner jet and inner radio lobes are shown with the green contours (Burns et al. 83), the NML as the yellow contours (Morganti et al. 99). The red circle denotes the approximate position of the HI cloud located at the base of the NML (Schiminovich et al. 94; Oosterloo & Morganti 05). The position of the active nucleus is shown with the black arrow. The approximate positions of the inner and outer optical filaments (Blanco et al. 75; Morganti et al. 99) are shown as the cyan lines.

Inner Lobes of Cen A

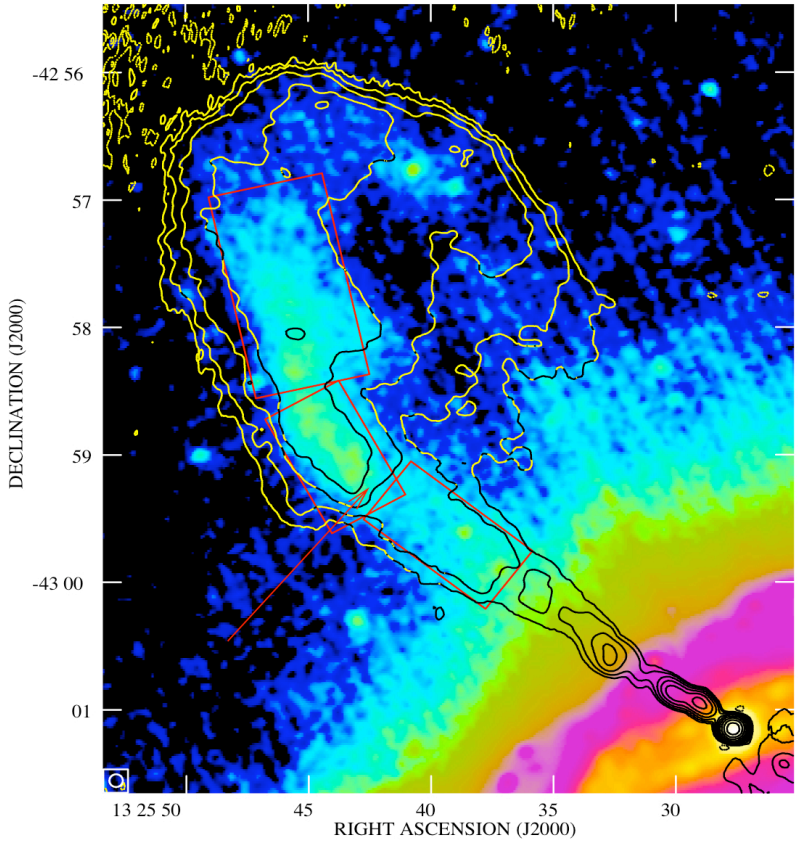

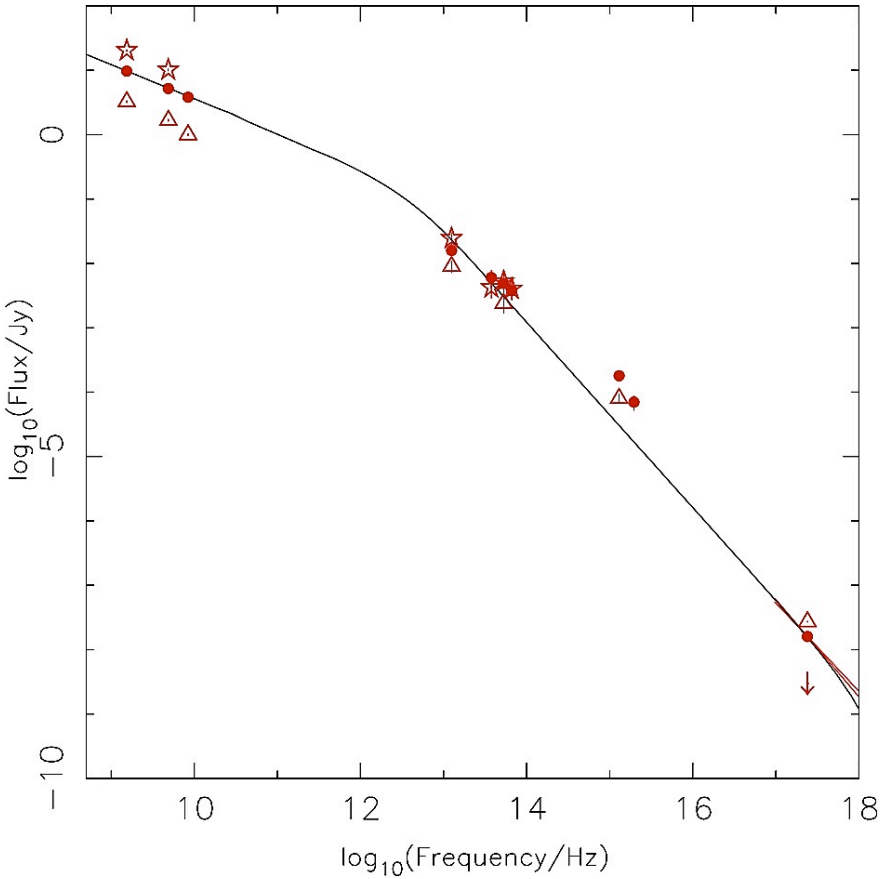

Hardcastle et al. 06:
[Left] 24 μm Spitzer image of the inner (Northern) lobe of Centaurus A radio galaxy, together with radio contours.
[Right] SEDs of the kpc-scale jet and inner lobe indicate that radio-to-X-ray continua are synchrotron in origin.
$B_{eq} \sim 30\ \mu G$ for the lobe.

Bow-Shock in Cen A

Croston et al. 09: Inner bow-shock around kpc-scale Southern lobe of Cen A emitting synchrotron X-rays.

d_{sh} ~ 300 pc, B_{eq} ~ 10 μG, p ~ 2 x 10^{-12} cgs, v_{sh} ~ 0.01c, γ_{max} ~ 10^8, t_{life} ~ 2 Myr, L_j ~ 10^{43} erg/s, M_{sh} ~ 8

Hillas criterium for UHECRs fulfilled only if B in shock is ~ 300 μG (~ 30 B_{eq}). Inverse-Compton emission may be however prominent in gamma-ray photon energy range.

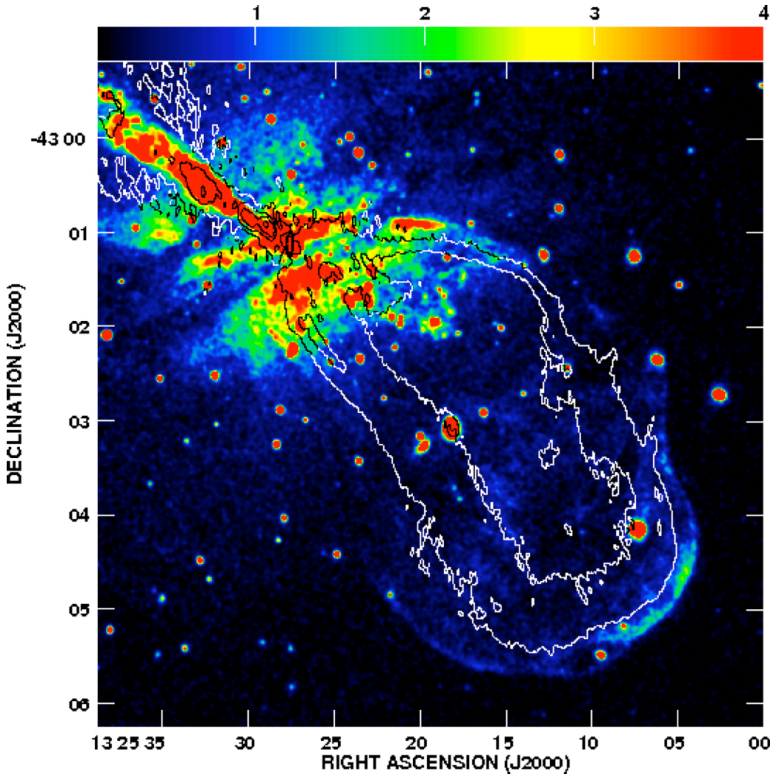

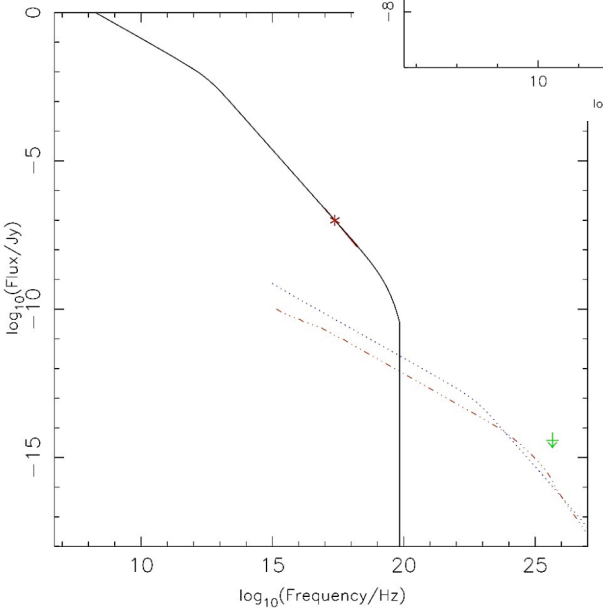

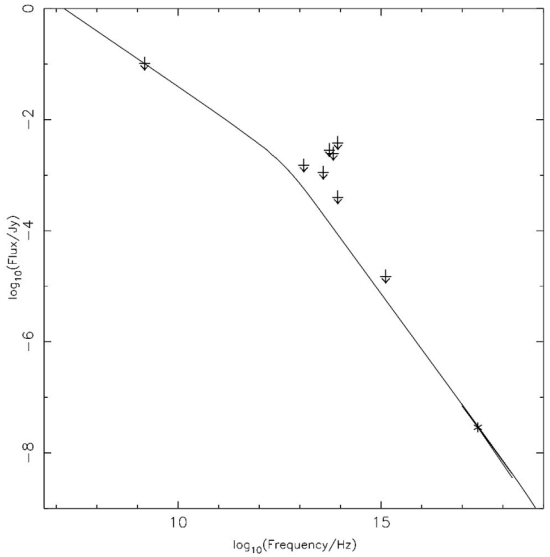

Bow Shock in Cygnus A

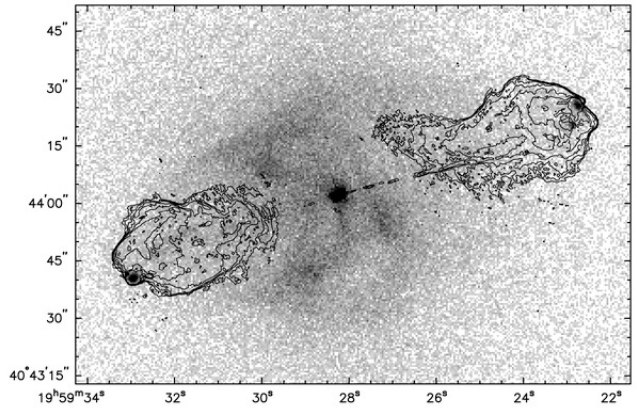

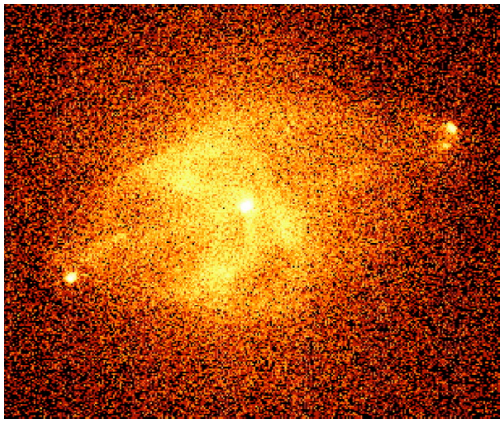

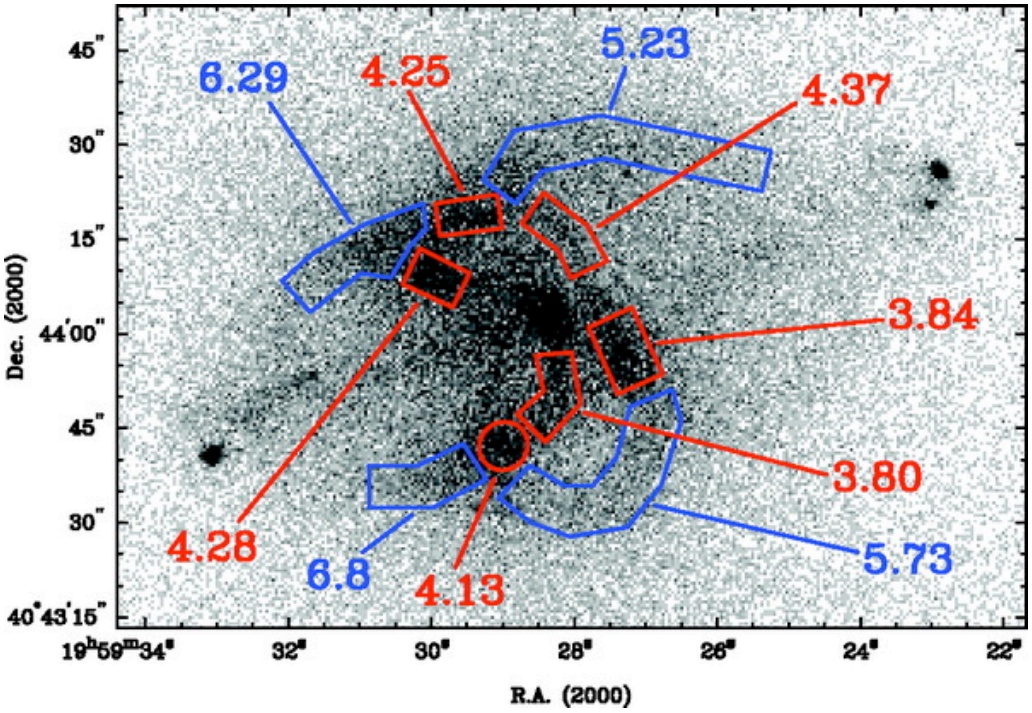

Wilson et al. 06: limb-brightened cavity of the radio galaxy Cygnus A, as revealed by the Chandra X-Ray Observatory. The gas along the north and south edges of the cavity is found to have an average temperature of 6.0 keV, which is hotter than the temperature (4.6 keV) of the adjacent intracluster gas. The shock is thus inferred to be weak (Mach number 1.3, a value also inferred from the density jump at the cavity edge), and its velocity is 0.003c. The total kinetic power of the expansion is found to be ~10^{46} ergs/s, which is somewhat larger than both the total radio power and the power emitted by the entire intracluster medium in the 2-10 keV band. It appears that most of the power of the jets in Cygnus A is currently going into heating the intracluster medium. From the derived pressure inside the cavity, there is no conclusive evidence for a component contributing pressure additional to the magnetic fields and ultrarelativistic electrons.

Bow Shock in Hercules A

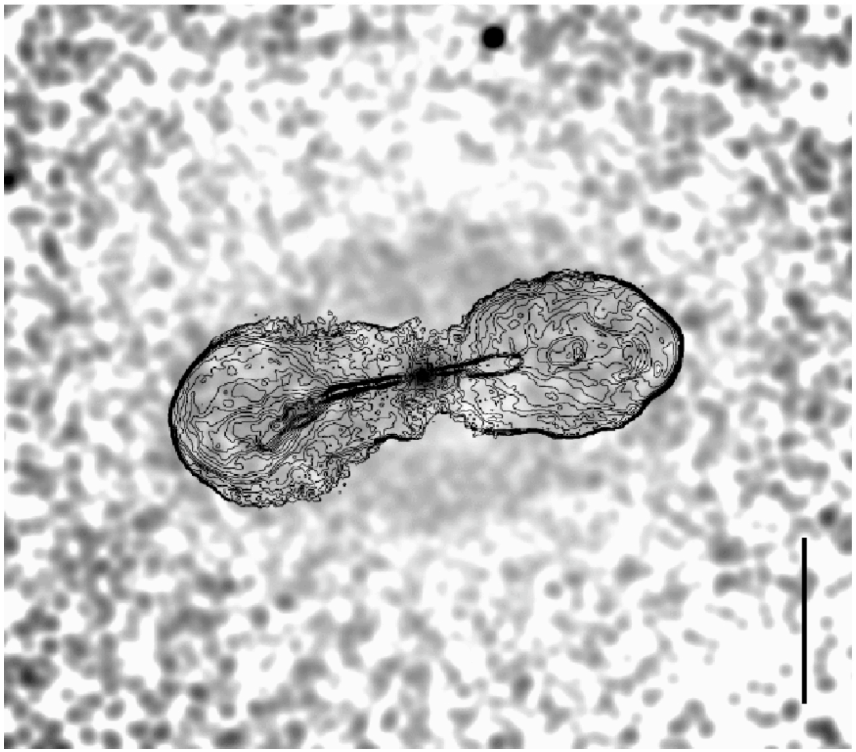

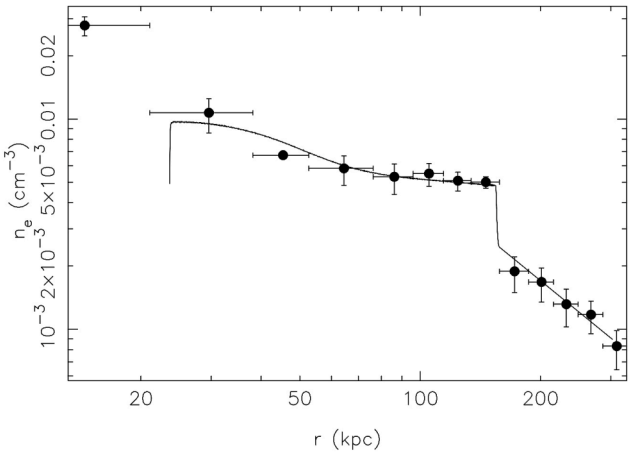

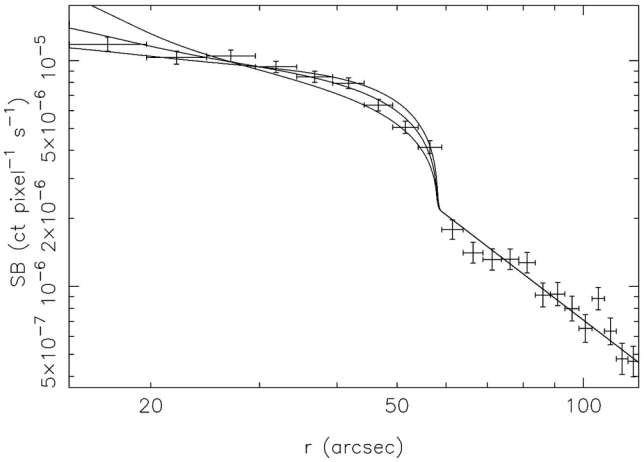

Nulsen et al. 05 : The radio source Hercules A resides at the center of a cooling flow cluster of galaxies. A Chandra X-ray image reveals a shock front in the intracluster medium (ICM) surrounding the radio source, about 160 kpc from the active galactic nucleus (AGN) that hosts it. The shock has a Mach number of 1.65, making it the strongest of the cluster-scale shocks driven by an AGN outburst found so far. The age of the outburst is ~60 Myr, its energy ~3 × 10^{61} ergs, and its mean power ~2 × 10^{46} erg/s.

Bow Shock in Hydra A

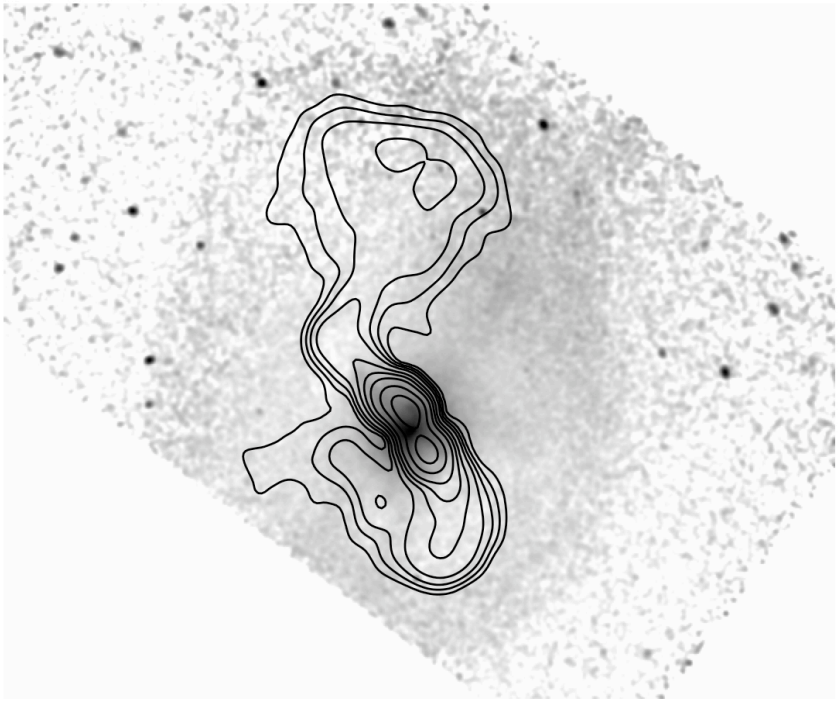

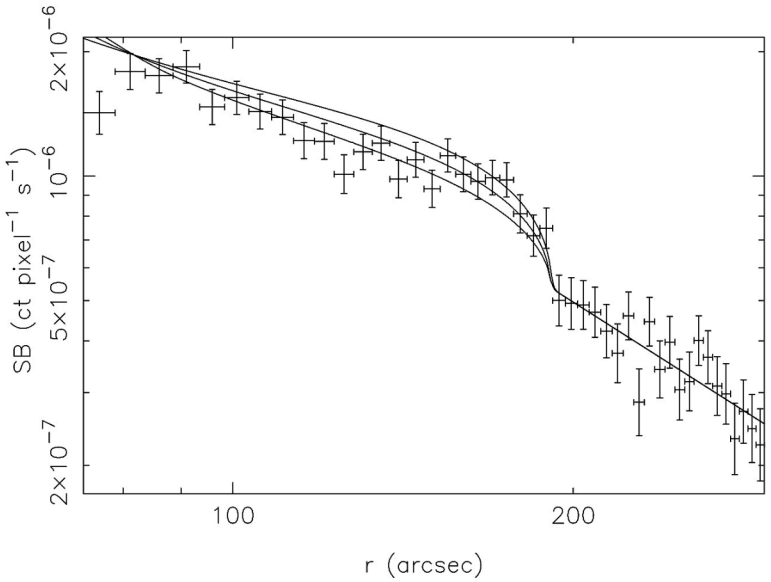

Nulsen et al. 05: Deep Chandra observations of the Hydra A Cluster reveal a feature in the X-ray surface brightness that surrounds the 330 MHz radio lobes of the AGN at the cluster center. Surface brightness profiles of this feature and its close association with the radio lobes argue strongly that it is a shock front driven by the expanding radio lobes. The Chandra image also reveals other new structure on smaller scales that is associated with the radio source, including a large cavity and filament. The shock front extends 200-300 kpc from the AGN at the cluster center, and its strength varies along the front, with Mach numbers in the range ~1.2-1.4. It is stronger where it is more distant from the cluster center, as expected for a shock driven by expanding radio lobes. Simple modeling gives an age for the shock front of ~100 Myr and a total energy driving it of ~10^{61} ergs.

Kpc-scale Gamma-ray Halos

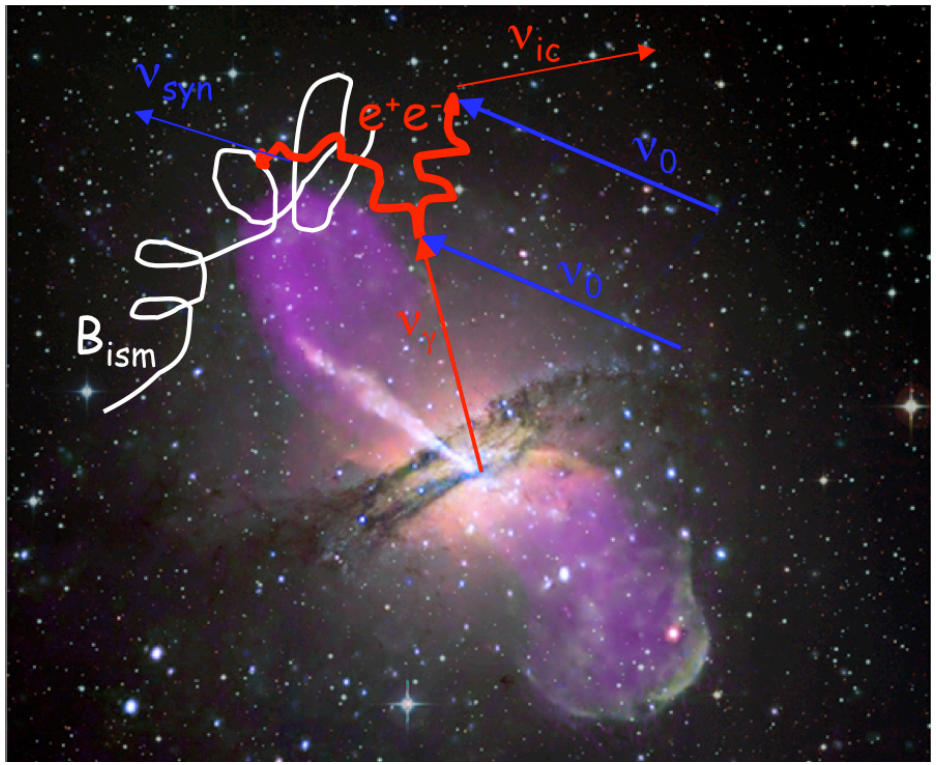

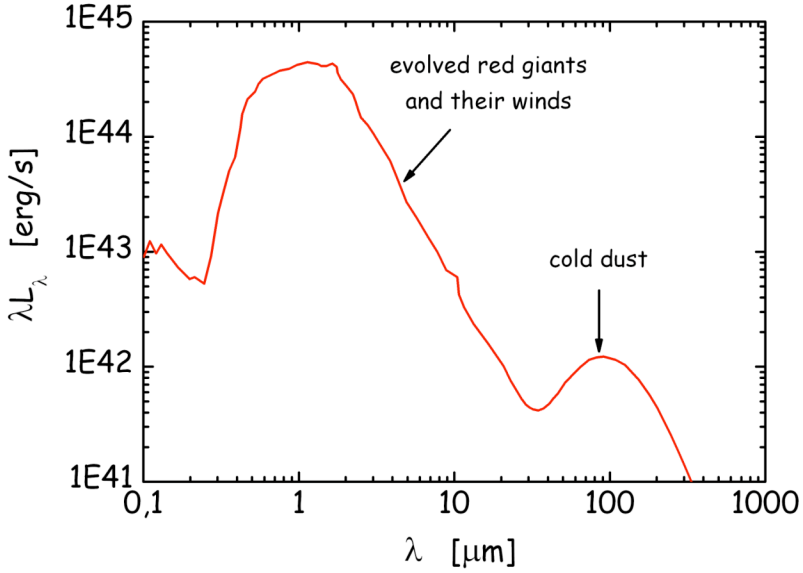

Stawarz et al. 06: about ~1% of the total, time-averaged TeV radiation produced by the active nuclei of low-power FR I radio sources is inevitably absorbed and re-processed by photon-photon annihilation on the starlight photon field, and the following emission of the created and quickly isotropized electron-positron pairs. In the case of the radio galaxy Centaurus A, the discussed mechanism can give a distinctive observable feature in the form of an isotropic gamma-ray halo. It results from the electron-positron pairs injected to the interstellar medium of the inner parts of the elliptical host by the absorption process, and upscattering starlight radiation via the inverse-Compton process mainly to the GeV-TeV photon energy range (see also Aharonian et al. 94).

Such a galactic gamma-ray halo is expected to possess a characteristic spectrum peaking at ~0.1 TeV photon energies, and the photon flux strong enough to be detected by modern Cherenkov Telescopes and, in the future, by GLAST. These findings should apply as well to the other nearby FR I sources.

Pair Halo in Cen A?

Aharonian et al. 09:
Cen A finally detected at TeV photon energy range.
Gamma-ray flux consistent with being steady on the timescale of months.

Optical image of Cen A overlaid with VLA radio contours. VHE best fit position with 1σ statistical errors (blue cross), and VHE extension upper limit (white dashed circle, 95% confidence level).

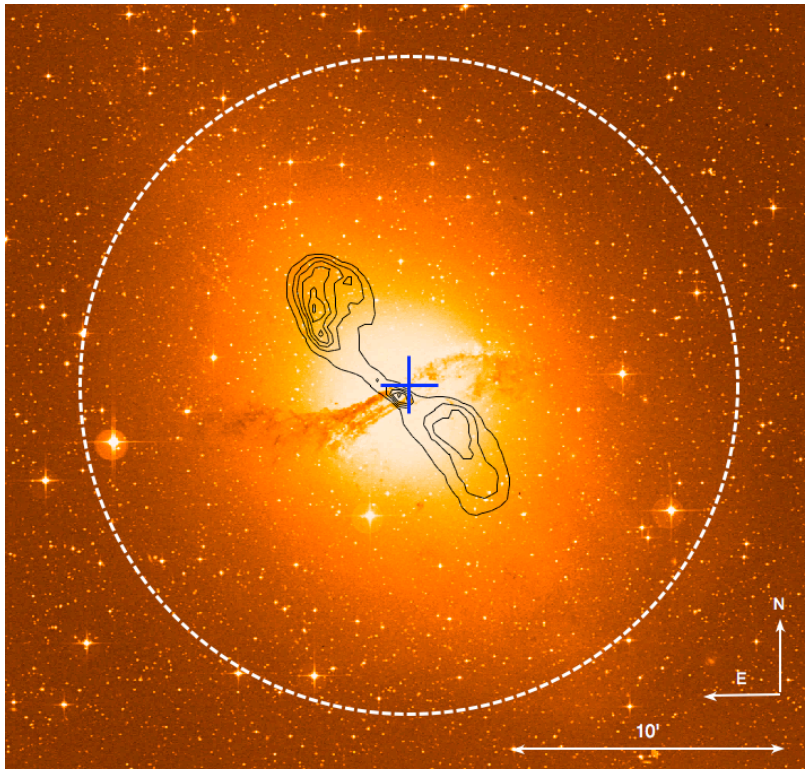

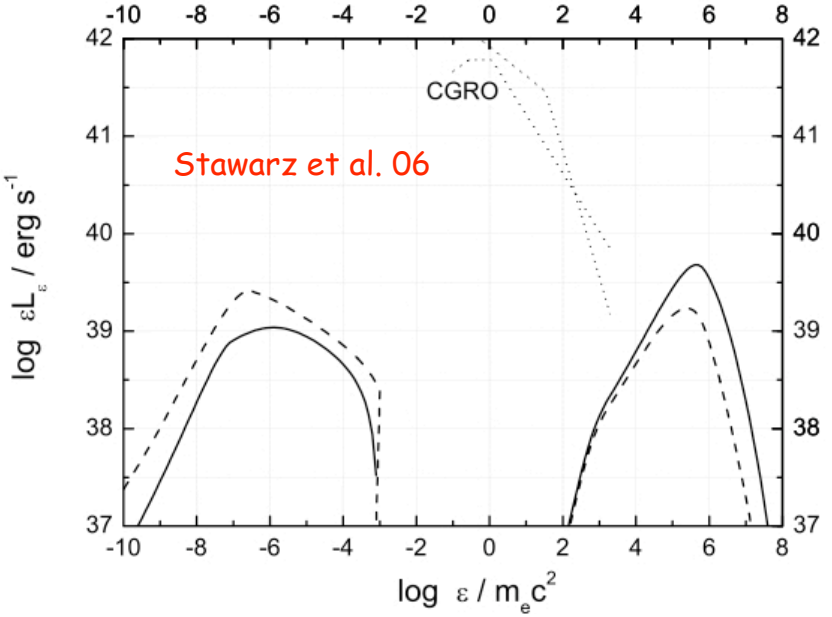

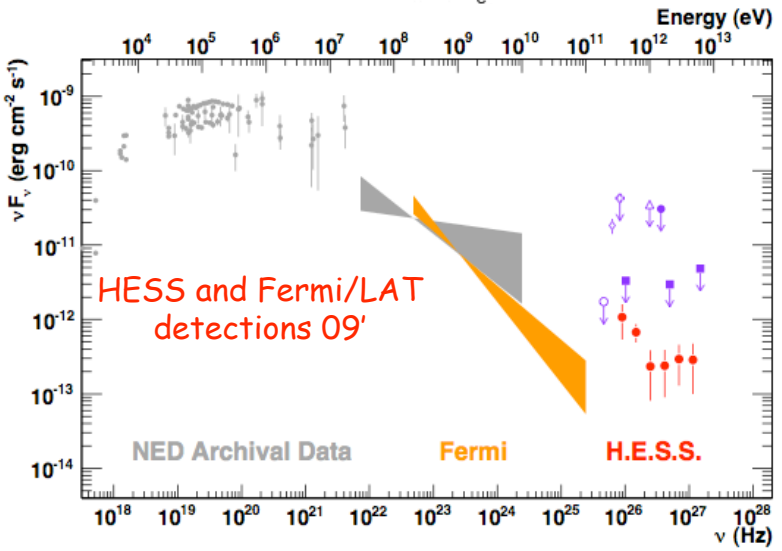

Gamma-ray Emission of M87

M87 radio galaxy has been detected at TeV photon energies by all IACTs (HEGRA, HESS, Magic, VERITAS; Aharonian et al. 03, 06, **Acciari et al. 08, 09**, Albert et al. 08), as well by Fermi/LAT at GeV photon energies (**Abdo et al. 09**).

Even though gamma-ray instruments cannot resolve different radio components of M87, the observed variability of the TeV emission indicates that it originates in the inner parts of the M87 jet rather than in the extended lobes.

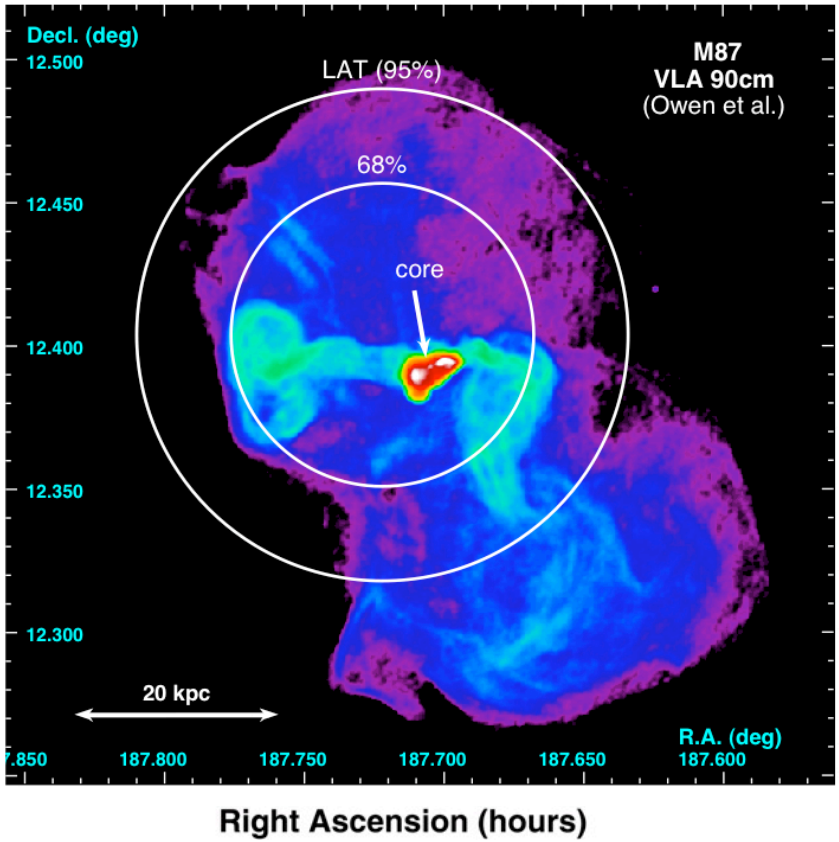

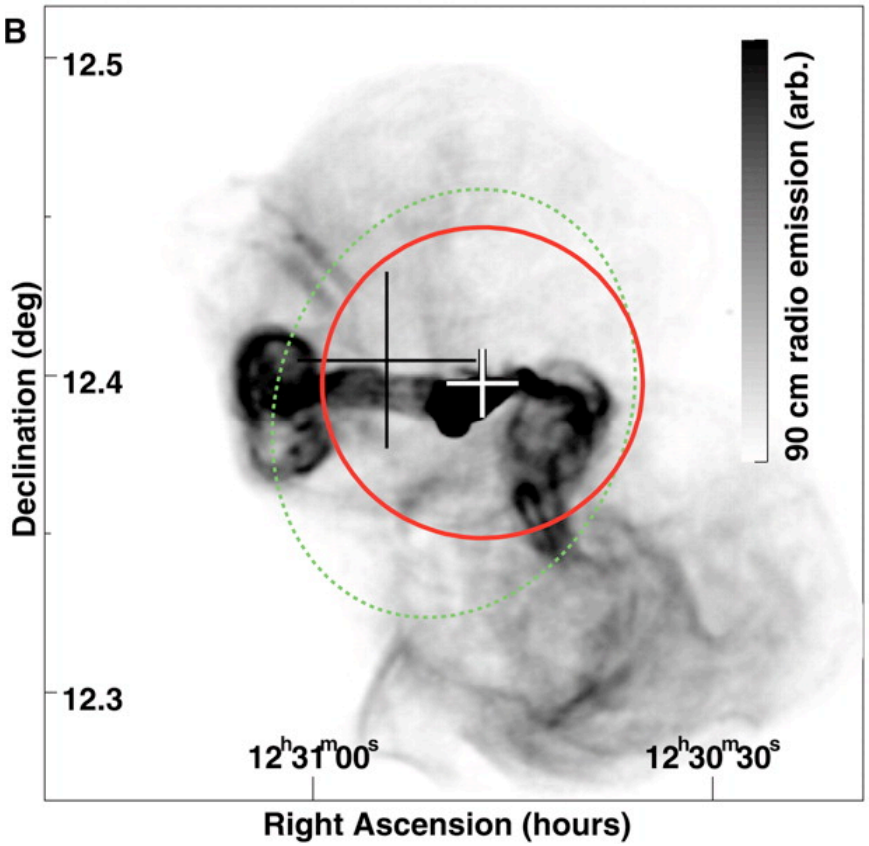

Inner Lobes of M87

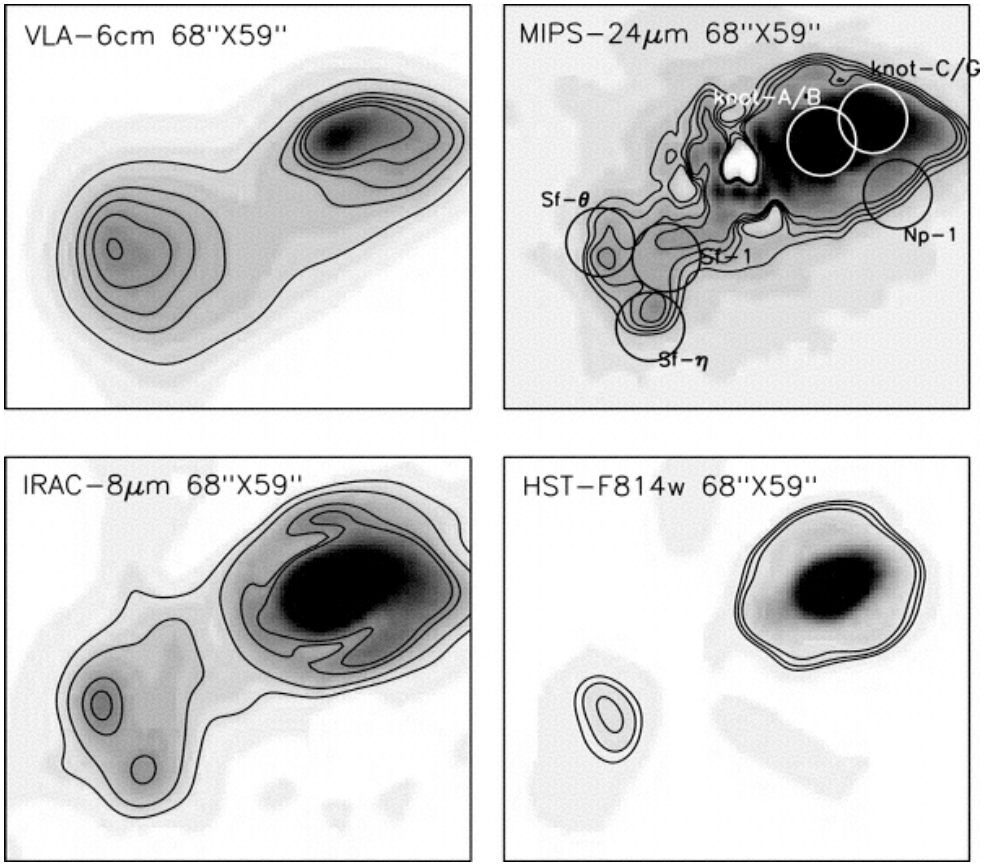

Shi et al. 07: The Spitzer data provide improved constraints on the synchrotron spectrum in the kpc-scale lobes of M87.
t_{syn} ~ 10^3 yrs, corresponding to the cooling length of 300 pc (4''). Therefore, in situ reacceleration of electrons must occur not only in M87 jet, but also within the lobes.

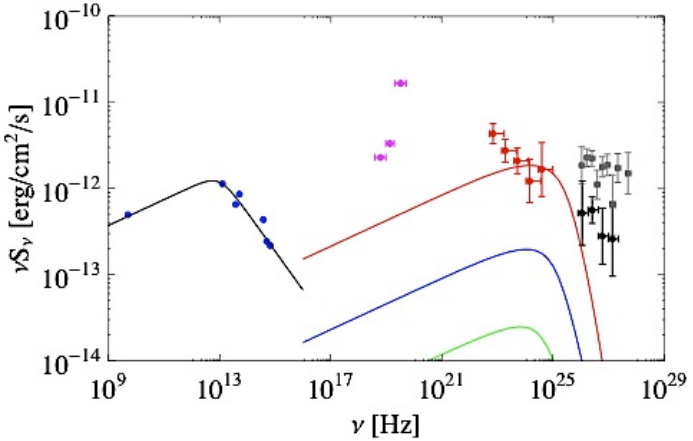

Kpc-scale lobes of M87 may contribute to the observed gamma-ray emission via IC/starlight process, but only if B < B_{eq} ~ 100 μG
(plot: $B_{eq}/3$, B_{eq}, $3B_{eq}$)

E_{tot} ~ 10^{55} erg (assuming energy equipartition), what implies the required jet power L_j ~ E_{tot}/t_{syn} ~ 3 × 10^{44} erg/s (in agreement with the constraints for the M87 jet; Bicknell & Begelman 96, Owen et al. 00). The gravitational potential as implied by the X-ray luminosity of the surrounding thermal gas is much lower than this. If the electrons within the lobes are reaccelerated in situ by a mechanism driven by the jet, most of the jet power must be converted into the radiating particles, and only a small fraction of the jet power is used to inflate a cavity (radio lobe) in the thermal gas atmosphere.

UHECRs Detected by PAO

Abraham et al. 07: Using data collected at the Pierre Auger Observatory during the first 3.7 years, a correlation between the arrival directions of cosmic rays with energy above ~ 6 x 10^{19} eV and the positions of AGN lying within ~ 75 Mpc is claimed. The hypothesis of an isotropic distribution of these cosmic rays may be rejected with at least a 99% confidence level from a prescribed a priori test. The claimed correlation is compatible with the hypothesis that the highest energy particles originate from nearby extragalactic sources whose flux has not been substantially reduced by interaction with the cosmic background radiation. AGN or objects having a similar spatial distribution are possible sources.

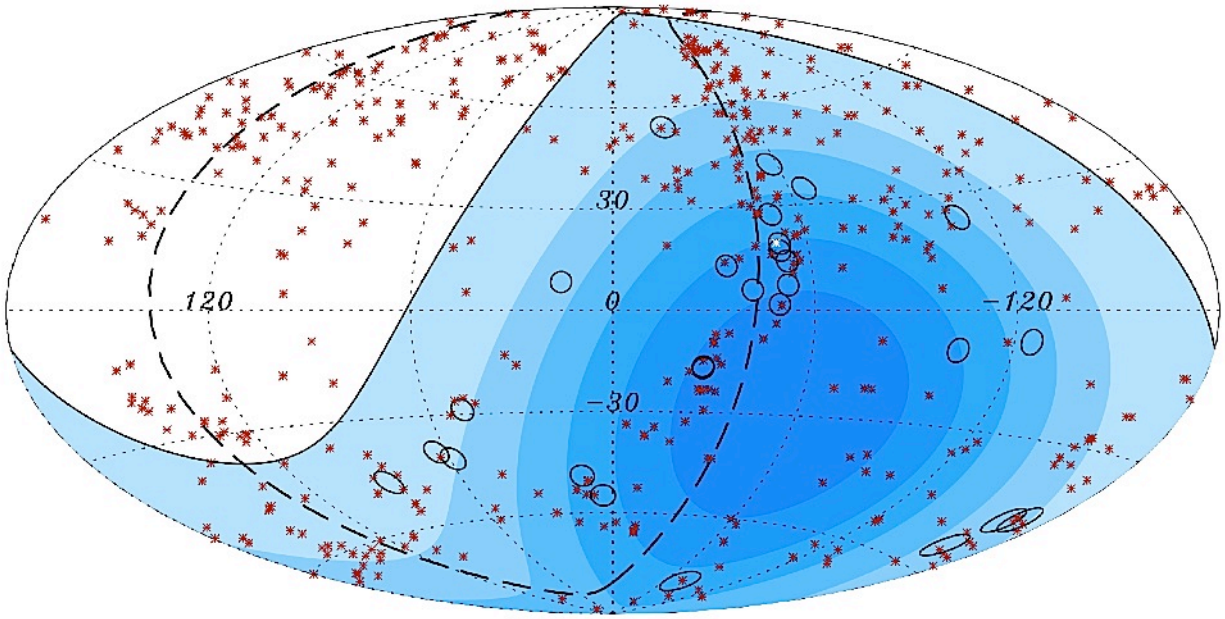

The positions of the 472 AGN (318 in the field of view of the PAO) with redshift z < 0.018 (D < 75 Mpc) from the 12th edition of the Veron-Cetty & Veron 06 catalog of quasars and active nuclei are indicated by red asterisks. The solid line represents the border of the field of view (zenith angles smaller than 60). Darker color indicates larger relative exposure. Each colored band has equal integrated exposure. The dashed line is the supergalactic plane.
Centaurus A, one of our closest AGN, is marked in white.

UHECR/AGN Connection?

Moskalenko et al. 09: A detailed study of the sample of AGN whose positions are located within 3.2deg of the UHECR events (and within 150 Mpc) shows that most of them are classified as Seyfert 2 and LINER galaxies whose properties do not differ substantially from other local AGN of the same type. Therefore, if the production of the highest energy CRs is persistent in nature, i.e., operates in a single object on long (>Myr) timescales, the claimed correlation between the CR events observed by PAO and the local active galaxies should be considered as resulting from a chance coincidence. Additionally, most of the selected sources do not show significant jet activity, and hence, in most conservative scenarios, there are no reasons for expecting them to accelerate CRs up to the highest energies, ~10^{20} eV (but see Pe'er et al. 09).

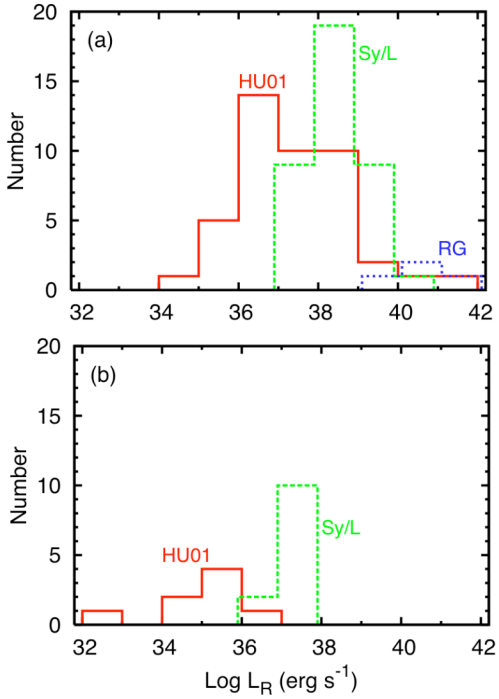

Number distributions of 5 GHz total radio powers (a), or upper limits for such (b), for Seyfert galaxies from the sample constructed by Ho & Ulvestad 01 (red solid), Seyfert/LINER possibly associated with UHECR events (green dashed), and radio galaxies possibly associated with UHECR events (blue dotted).

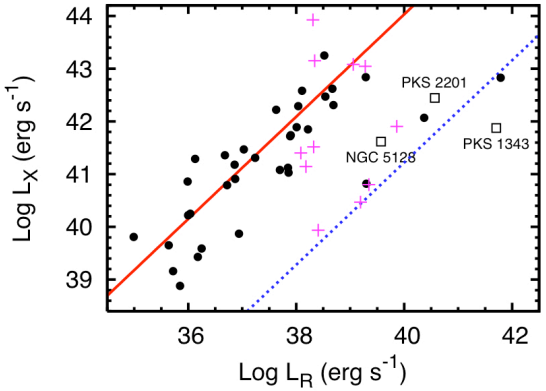

X-ray (2–10 keV) luminosity vs. 5 GHz total luminosity for Seyfert galaxies from the sample constructed by Panessa et al. 07 (black circles), Seyfert/LINER galaxies from our sample (magenta crosses), and radio galaxies from our sample (open squares). Red solid line indicates the best fit log L_X = 0.97 log L_R + 5.23 for Seyfert galaxies, and blue dotted line denotes the best fit log L_X = 0.97 log L_R + 2.42 for low-luminosity radio galaxies, both as given by Panessa et al.

60 μm luminosity vs. 5 GHz total luminosity for Seyfert galaxies from the sample constructed by Roy et al. 98 (detections: black circles, upper limits: open circles), Seyfert/LINER galaxies from our sample (magenta crosses), and radio galaxies from our sample (open squares).

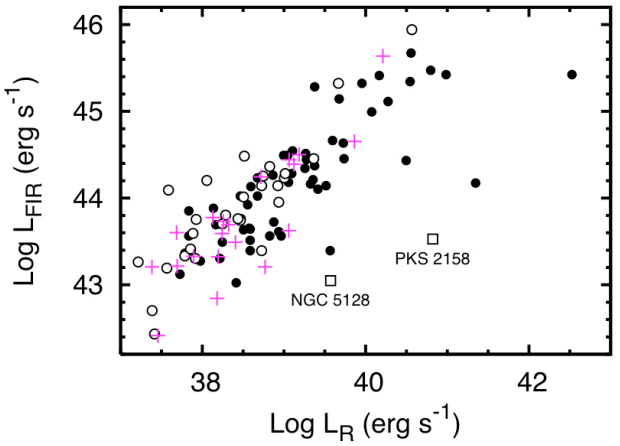

UHECRs From Nearby RGs?

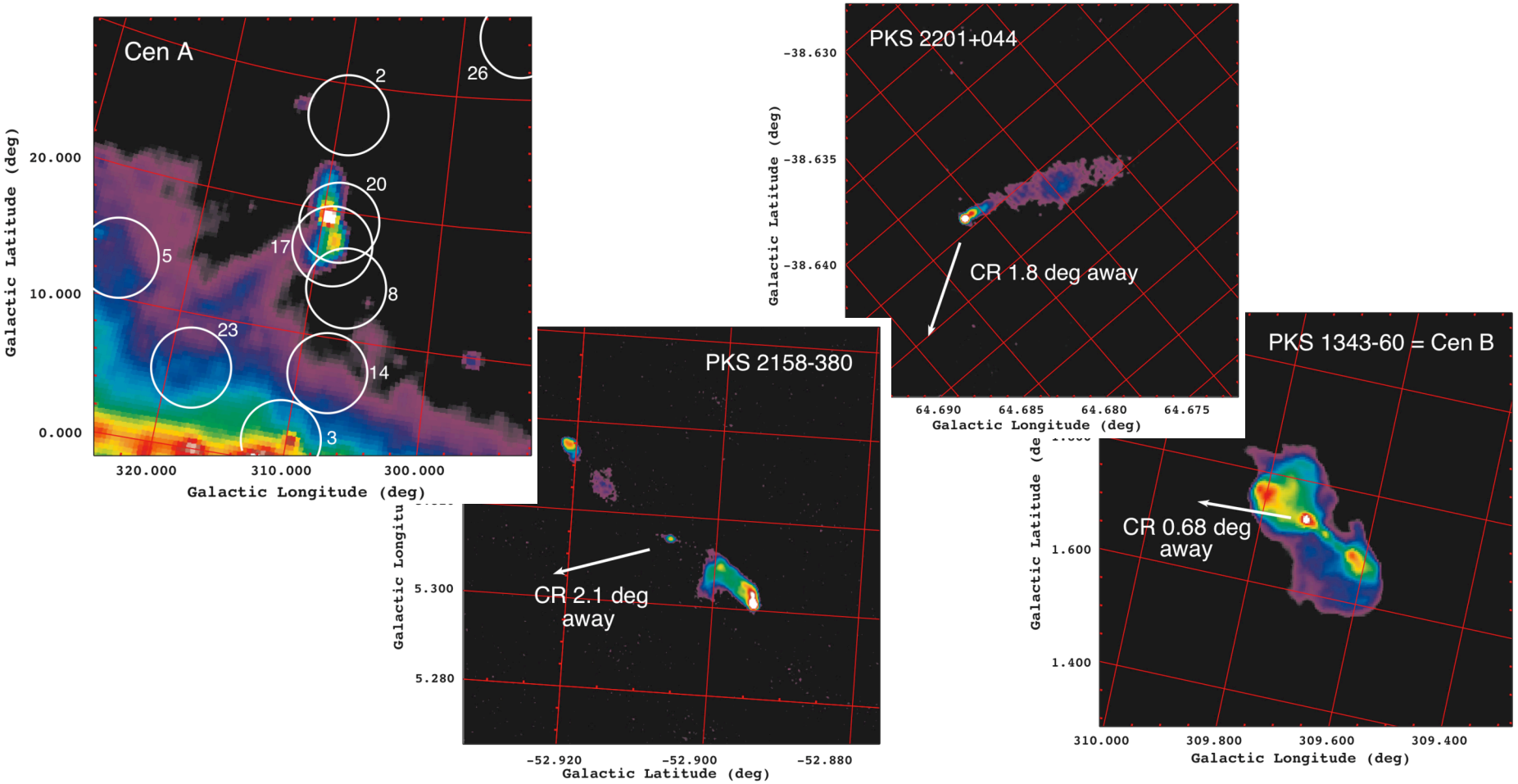

Moskalenko et al. 09: nearby radio galaxy Cen A alone could be associated with at least four events due to its large radio extent, and PKS 1343–60 (Cen B), another nearby radio galaxy, can be associated with more than one event due to its proximity to the Galactic plane and, correspondingly, the stronger Galactic magnetic field UHECRs encounter during propagation to the Earth. If the UHECRs associated with these events are indeed accelerated by Cen A and Cen B, their deflection angles may provide information on the structure of the magnetic field in the direction of these putative sources.

Mpc-scale Gamma-ray Halos?

Atoyan & Dermer 08:
UHECRs accelerated in the jets of active galactic nuclei can accumulate in high magnetic field, ~100 kpc-scale regions surrounding powerful radio galaxies. Photohadronic processes involving UHECRs and photons of the extragalactic background light make ultra-relativistic electrons and positrons that initiate electromagnetic cascades, leading to the production of a gamma-ray synchrotron halo.

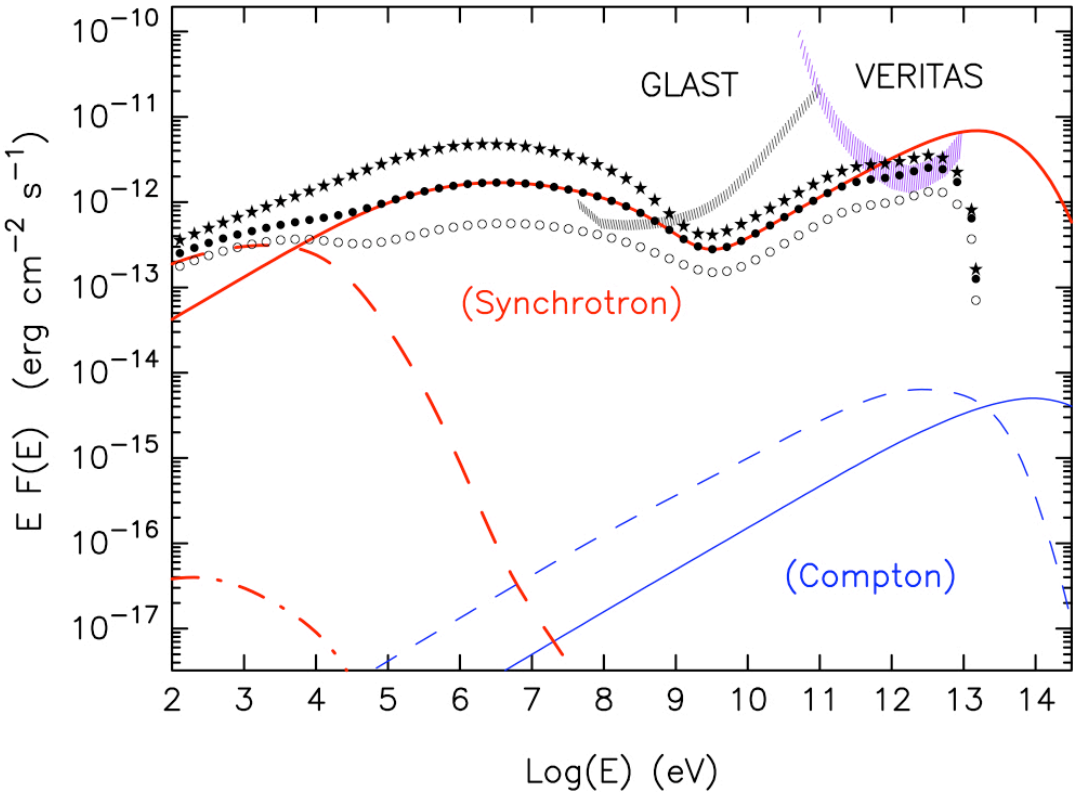

Fluxes from the electromagnetic cascade initiated within 0.5 Mpc distances from the core of Cyg A, assuming an average magnetic field B = 20 μG in the cavity. The total injection power of UHECR protons is 4×10^{46} erg/s. The photon fluxes expected for t_{age} = 30 Myr, 100 Myr and 300 Myr are shown by the open dots, full dots and stars, respectively. The solid, dashed, and dot-dashed curves show three generations of synchrotron (heavy curves) and Compton (light curves) cascade radiations in the case of 100 Myr. Note that the third generation of Compton cascade radiation is too weak to appear on the plot. Sensitivities for the FGST and VERITAS are also shown.

Relativistic Protons in Lobes?

Hardcastle & Worrall 00: Using ROSAT observations, gas pressures in the X-ray-emitting medium surrounding 63 FRII radio galaxies and quasars were estimated. These were compared with the internal pressures of the radio-emitting plasma estimated by assuming minimum energy condition. In the majority of cases radio sources appeared to be under-pressured with respect to the external medium. Non-relativistic particles (electrons and protons) are not likely to contribute significantly to the lobes' pressure (polarization studies!).

Figure 1. Plot of central thermal pressure against minimum pressure for the X-ray observed sources. The solid line shows equality of internal and external pressure. Most sources lie above it. Crosses denote sources with $z < 0.3$, and stars sources with $z > 0.3$. Arrows denote upper limits on thermal pressure; upper limits are plotted in light grey.

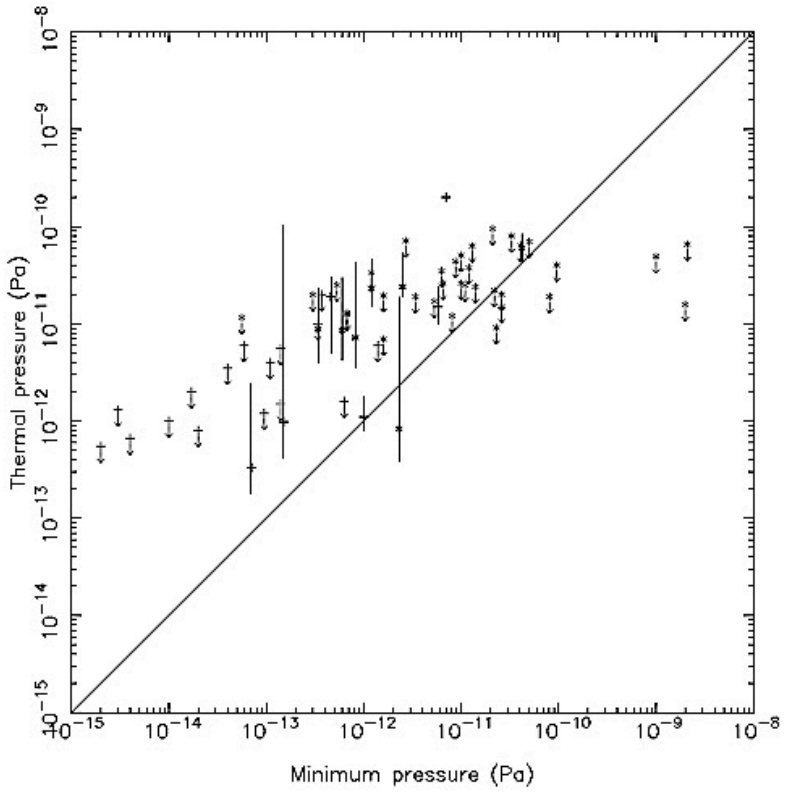

Figure 2. The ratio between central thermal pressure and minimum pressure as a function of lobe length. (Lengths plotted for the sources for which minimum pressure is calculated for the whole source are half the source length.) The solid line shows equality of internal and external pressure. Crosses denote sources with $z < 0.3$, and stars sources with $z > 0.3$. Arrows denote upper limits on thermal pressure; upper limits are plotted in light grey. The correlation seen in this figure arises mainly because of a strong anticorrelation between minimum pressure and source size.

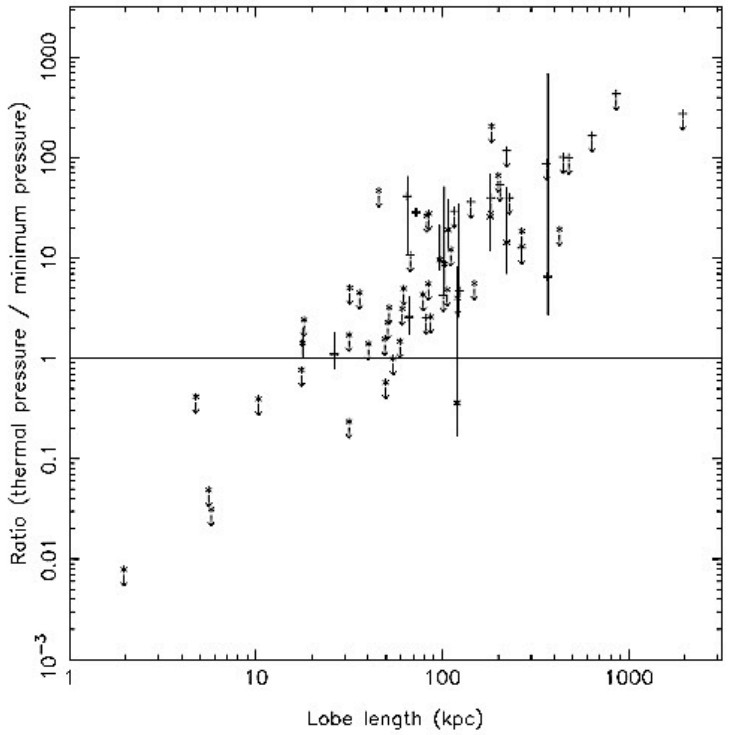

Lobes in Galaxy Clusters

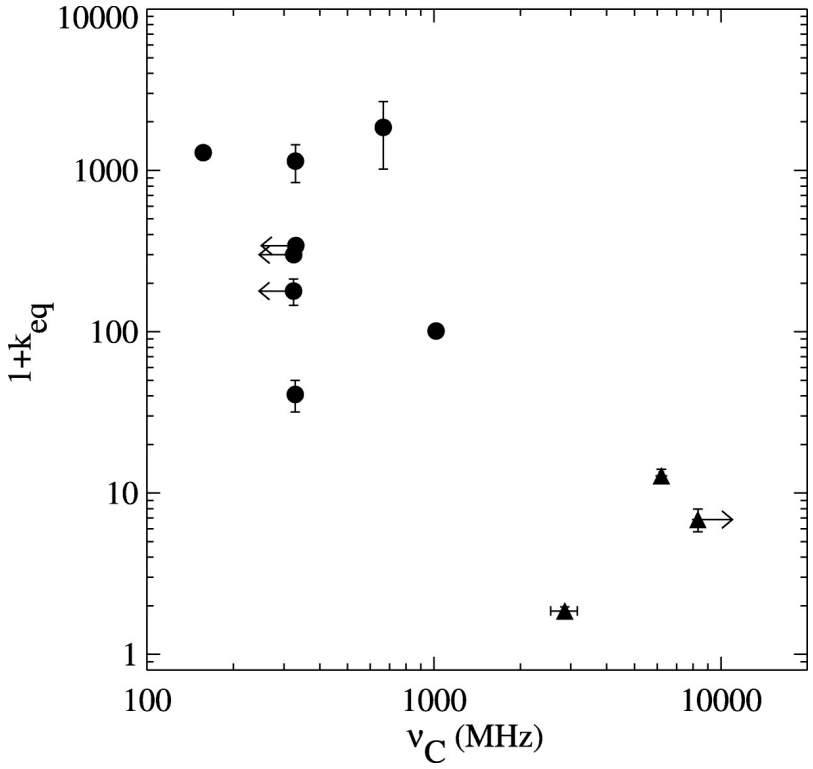

Birzan et al. 08: the magnetic field strengths within the kpc-scale lobes of low-power radio galaxies located at the centers of clusters vary between a few to several tens of μ G depending on the age and dynamical state of the lobes. If the cavities are maintained in pressure balance with their surroundings and are supported by internal fields and particles in equipartition, the ratio of energy in electrons to heavy particles (k) must vary widely from approximately unity to 4000, consistent with heavy (hadronic) jets.

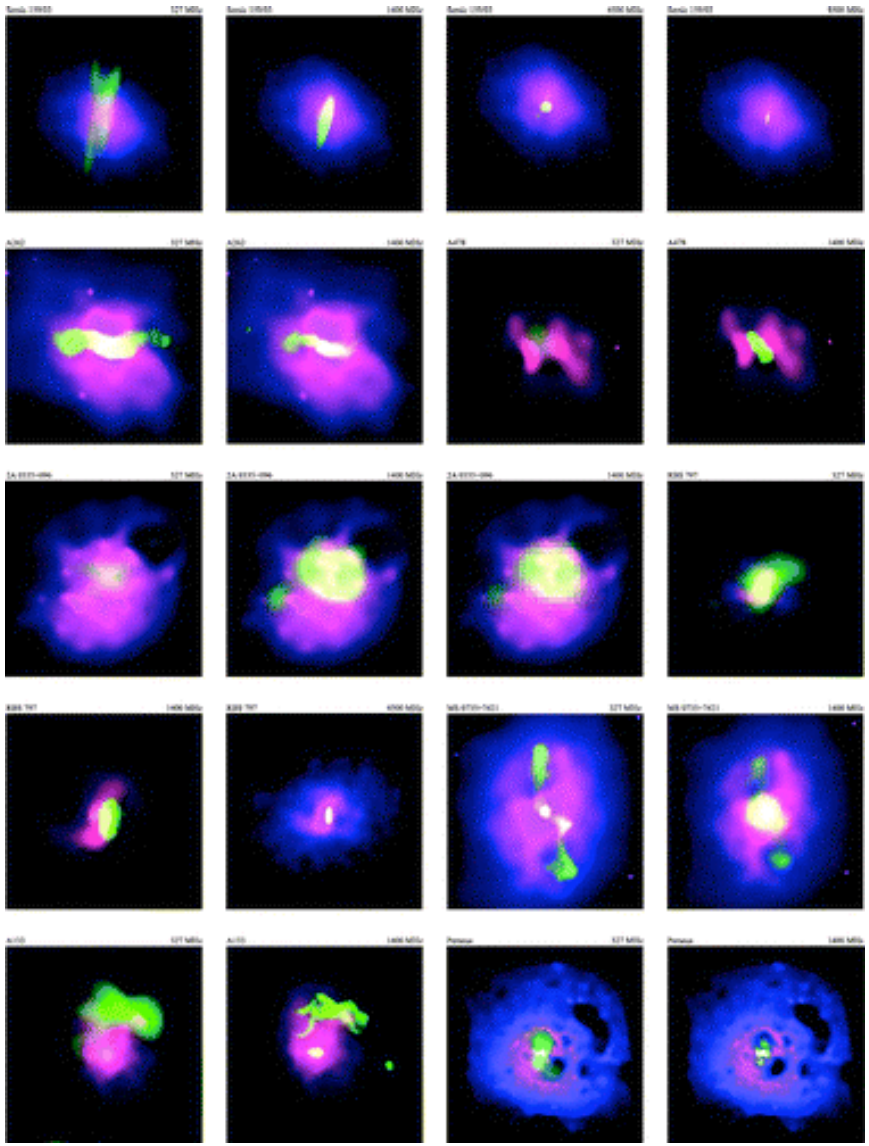

Jet Boundary Acceleration

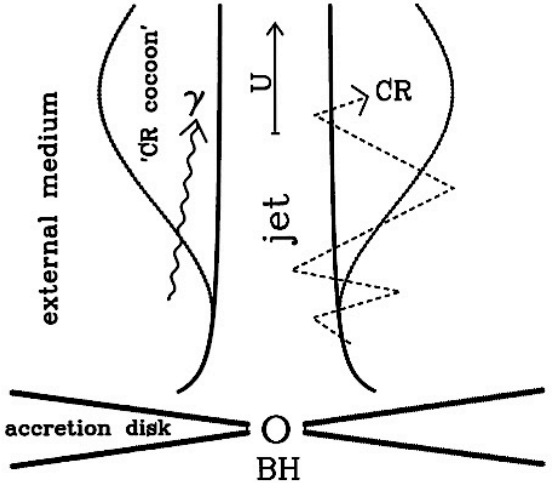

Ostrowski 90, 98, 00

Acceleration of relativistic protons at the boundaries of relativistic jets may provide flat-spectrum population of cosmic rays (UHECRs) within the lobes, leading to formation of over-pressured `cosmic-ray cocoons' around large-scale outflows, and gradual jet deceleration (see also Ostrowski & Sikora 01).

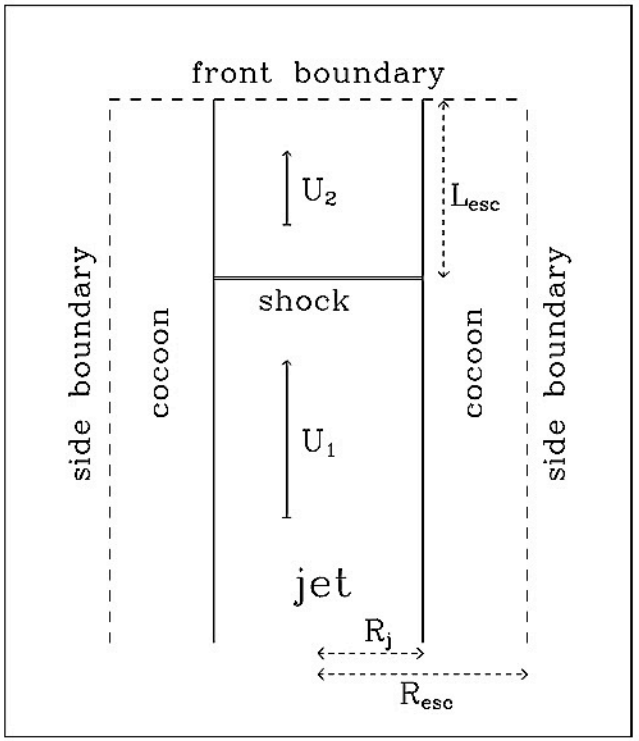

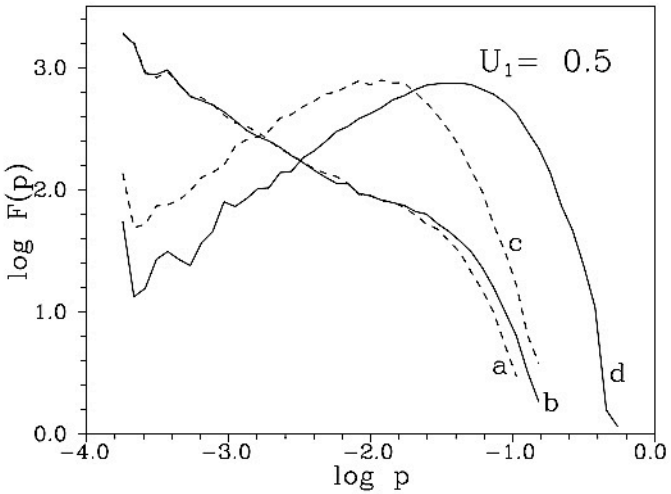

FIGURE 1. Comparison of the escaping particle spectra formed with wide (full lines 'b' and 'd') and narrow (dashed lines 'a' and 'c') turbulent cocoon surrounding the jet (cf. Ostrowski 1998). The results are presented for two possible particle injection sites: at the terminal shock (cases 'a' and 'b'), and far upstream the shock (cases 'c' and 'd'), where only the boundary acceleration is effective. Spectra of escaping particles are presented, the ones diffusively escaping from the cocoon (mostly in 'c' and 'd') and these advected downstream the terminal shock (mostly in 'a' and 'b'). Particle momentum unit is chosen in a way to give its gyroradius equal the jet radius at $p = 1$. Initial spectrum fluctuations appear near the injection momentum.

Sources of Relativistic Protons

1) Large-scale jets (acceleration at the jet boundary; **Ostrowski 90, 98, 00, Rieger & Duffy 04, Lyutikov & Ouyed 07**).

2) Stochastic acceleration within the lobes (**Fraschetti & Melia 08, Hardcastle et al. 09; but see O'Sullivan et al. 09, Lemoine & Waxman 09**).

For the particular case of Cen A giant lobes and UHECRs detected by PAO, the Hillas criterium $r_L < R$ is fulfilled. Here

$$r_L = E_p / e B \sim 100\ (E_p/100\ \mathrm{EeV})\ (B/\mu G)^{-1}\ \mathrm{kpc}$$

is the particle gyroradius, and $R \sim 100$ kpc is the lobes' radius. This criterium, for the assumed optimistic acceleration timescale

$$t_{acc} \sim 10\ r_L / c \sim 3\ (E_p/100\ \mathrm{EeV})\ (B/\mu G)^{-1}\ \mathrm{Myr},$$

is equivalent to the condition $t_{acc} \sim t_{esc}$, where the escape timescale is

$$t_{esc} \sim 3\ R^2 / r_L\ c \sim (E_p/100\ \mathrm{EeV})^{-1}\ (B/\mu G)\ \mathrm{Myr}.$$

Note that the lobes' lifetime is much longer than this, $t_{life} \sim 30$ Myr.
In addition, with 4 UHECR events possibly associated with Cen A, the total UHECR luminosity $L_{UHECR} \sim 10^{39}$ erg/s, is much lower than the total jet kinetic power in this source, $L_j \geq 10^{43}$ erg/s.

3) Extended bow shocks (**Berezhko 08, Croston et al. 09**).

This scenario requires very efficient amplification of the magnetic field at the shock front. In the particular model by Berezhko 08, the maximum available proton energy is

$$(E_p/100\ \mathrm{EeV}) \sim (L_j/10^{46}\ \mathrm{erg/s})^{3/4}\ (n_g/10^{-4}\mathrm{cm}^{-3})^{-1/4}\ (v_{sh}/0.3c)^{-1/4}\ (LS/\mathrm{kpc})^{-1/2}$$

Conclusions

1) Extended (kpc - Mpc) lobes in radio galaxies and quasars are confirmed sources of high-energy (X-ray and gamma-ray) radiation.

2) Maximum energies of ultrarelativistic electrons within extended lobes are of the order of 0.1 TeV. Magnetic field intensities thereby are of the order of 1-100 μG.

3) There are several indications for the in situ particle acceleration and for the dynamical role of ultrarelativistic protons within the extended lobes.

4) Extended lobes of nearby radio galaxies are likely sources of ultra high energy cosmic rays, with the observed energies of the order of 10-100 EeV.

5) Relativistic jets, turbulence, and bow shocks within and around extended lobes of radio galaxies and quasars may accelerate protons to the highest observed energies.